Land Reclamation Controls on Multi-Centennial Estuarine Evolution

R.A. Schrijvershof[1,2], D.S. van Maren[2,3], M. van der Wegen[2,4], A.J.F. Hoitink[1]

[1]Wageningen University & Research, Environmental Sciences Group, Wageningen, The Netherlands
[2]Deltares, Delft, The Netherlands
[3]Delft University of Technology, Faculty of Civil Engineering and Geosciences, The Netherlands
[4]IHE-Delft Institute for Water Education, Delft, The Netherlands

Key Points:

- Land reclamation in the Ems estuary has led to progressive subtidal infilling and degeneration of separated ebb-flood channels
- Loss of intertidal areas distorts the estuary-scale channel-flat configuration, which is partly restored by subtidal infilling
- Tidal asymmetry-based equilibrium theory can predict the evolutionary trajectory of real-world estuaries responding to land reclamation

Corresponding author: R.A. Schrijvershof, reinier.schrijvershof@wur.nl,reinier.schrijvershof@deltares.nl

Abstract

Land reclamations influence the morphodynamic evolution of estuaries and tidal basins, because altered planform changes tidal dynamics and associated residual sediment transport. The morphodynamic response time to land reclamation is long, impacting the system for decades to centuries. Other human interventions (e.g., deepening of fairways or port construction) add a morphodynamic adaptation timescale to a system that may still adapt as the result of land reclamations. Our understanding of the cumulative effects of anthropogenic interference with estuaries is limited, because observations usually do not cover the complete morphological adaptation period. We aim to assess the impact of land reclamation works and other human interventions on an estuarine system by means of digital reconstructions of historical morphologies of the Ems Estuary over the past 500 years. Our analysis demonstrates that the intertidal-subtidal area ratio altered due to land reclamation works and that the ratio partly restored after land reclamation ended. The land reclamation works have led to the degeneration of an ebb- and flood channel system, transitioning the estuary from a multichannel to a single-channel system. We infer that the 20^{th}-century intensification of channel dredging and re-alignment works accelerated rather than cause this development. The centennial-scale observations suggest that estuarine systems responding to land reclamations follow the evolutionary trajectory predicted by tidal asymmetry-based stability theory as they move towards a new equilibrium configuration with modified tidal flats and channels. Existing estuarine equilibrium theory, however, fails in linking multichannel stability to the loss of intertidal area, emphasizing the need for additional research.

Plain Language Summary

Reclaiming land along the margins of estuaries and tidal basins leads to loss of intertidal areas. The response of the remaining underwater landscape to the loss of intertidal areas takes decades to centuries. This impacts the patterns, dimensions, and functionalities of the channels and tidal flats. Observations are usually not available for such a long period, limiting our capacity to study the impact of land reclamation. Here, we overcome this limitation by reconstructing the landscape adaptation in the Ems estuary since land reclamation accelerated in the beginning of the 16^{th} century, when storms reshaped the estuary. Historical and recent topo-geographical sources were used to reconstruct the centennial-scale developments of the tidal channels and tidal flats. Results show that, after reclamation works stopped, the tidal flats reduced in area and the tidal channels filled up. The tidal channel patterns and dimensions permanently changed, impacting, for example, shipping waterways. Further research should address the link between changes in intertidal areas and channel dynamics because we currently lack such a comprehensive understanding. This hampers our ability to predict the effects of future anticipated tidal flat changes, as a result of, for example, sea level rise or tidal flat restoration works.

1 Introduction

Estuaries and tidal basins are biodiverse coastal landscapes that are often intensely used by humans, offering services such as navigation routes, fisheries, and protection against flooding. These services are provided by estuarine morphology because the channel-flat pattern and geometry (hypsometry) determine hydrological connectivity (Hiatt & Passalacqua, 2015), ecological connectivity (Olds et al., 2017), and influences future morphodynamic evolution because of the link with tidal asymmetry and residual sediment transport (Dronkers, 1986; Z. Wang et al., 1999). Large-scale human alteration of estuarine planform and channel dimensions influences tidal dynamics, sediment transport, and ultimately the basin's long-term evolution. Engineering works and construction of embankments restrain intertidal dynamics. This process of "coastal squeeze" affects the accommodation space available for dynamic adaptation to sea level rise (Borchert et al., 2018). Understanding and predicting the combined impact of global climate change and anthropogenic pressure requires grasping the complex interaction between the tidal channels and the adjacent intertidal areas (Z. B. Wang et al., 2015; Hoitink et al., 2020).

Tidal channels dynamically interact with tidal flats and associated salt marshes. Tidal flat development influences tidal propagation characteristics (Dronkers, 1986) and channel mobility (Kleinhans et al., 2022), which in turn affect the channel dynamics and the system-scale morphodynamic development (A. Hibma et al., 2004; van der Wegen et al., 2008; Braat et al., 2017; Leuven & Kleinhans, 2019). Important hydrodynamic mechanisms linked to the tidal flats are the temporal storage of mass and dissipation of momentum (Friedrichs & Aubrey, 1988; Alebregtse, 2015; Zhou et al., 2018). Both influence tidal propagation, leading to asymmetric sea surface elevations and velocity distribution (e.g., Friedrichs, 2010). An asymmetric tidal motion drives a net sediment transport flux (Groen, 1967; Van de Kreeke & Robaczewska, 1993), while the long-term, residual transport determines morphological evolution (Dronkers, 1986). Large-scale changes in the channel-flat configuration therefore disrupt the net sediment transport magnitudes and directions (import versus export) and steer the morphodynamic evolution of an estuary or tidal basin (Van Der Wegen, 2013; Guo, Zhu, et al., 2022; Chen et al., 2020).

In many tidal systems worldwide, the loss of intertidal area due to land reclamation and channel deepening due to dredging have been the major anthropogenic interferences over the past and present century (Talke & Jay, 2020). The construction of embankments (artificial levees) for flood protection and land reclamation purposes effectively alters the tidal regime, because the basins' geometry (i.e.; depth, width, length) is essentially changed (Talke & Jay, 2020). Tidal flat loss reduces the embayments' intertidal storage volume, decreasing the tidal prism and enhancing flood dominance (Speer & Aubrey, 1985). An increased sediment import will lead to basin infilling, which will continue until the channel geometry has re-established to new equilibrium conditions, in which the sediment transport capacity can maintain the new channel-flat configuration (Dronkers, 2016). Tidal-asymmetry based equilibrium theory can be useful to assess the evolutionary trajectory of an estuarine system responding to land reclamations (Zhou et al., 2018).

The morphodynamic response to large-scale interventions, such as tidal flat reclamation is, however, often slow and manifests itself on longer time-scales (Guo, Zhu, et al., 2022). The response time depends on the magnitude of the intervention, the size of the system, and the sediment transport rates, and may typically be several decades or more (van Maren, Colina Alonso, et al., 2023). Various concurrent human interventions (reclamation, deepening, construction of hydraulic works) may impact a system. It is difficult to isolate the impact of a single intervention because each intervention adds a morphodynamic adaptation timescale to a system that may still adapt as the result of previous interventions. As a result, multiple interventions may interactively impact the system within the morphodynamic adaptation time, possibly exacerbating or accelerating the system's response to the principle intervention (Z. B. Wang et al., 2015).

Land reclamation and channel deepening may influence system-scale sediment budgets (Guo, Xie, et al., 2022; Donatelli et al., 2018), initiate a transition to hyper-concentrated flow conditions (Winterwerp et al., 2013; Van Maren, Winterwerp, & Vroom, 2015; Van Maren et al., 2016), and influence channel migration and avulsion (Dai et al., 2016). In the Ganges-Brahmaputra-Meghna (GBM) mega delta, for example, large-scale land reclamation (>5000 km^2) in the 60's and 70's of the 20^{th} century has led to a significant change in the hydro-sedimentary regime, drastically increasing flood risk (Auerbach et al., 2015), persistent infilling of the tidal channels (Wilson et al., 2017), and, as a result, a reorganization of the tidal channel network (Bain et al., 2019; van Maren, Beemster, et al., 2023). Such large-scale human interventions may thus impact delta system functioning for decades to centuries through non-linear feedback loops, exceedance of thresholds, and time-lags (Liu et al., 2007; Coco et al., 2013). The observed and widely varying impact of land reclamation can not be predicted on the basis of estuarine equilibrium theory. To date, it remains unclear to what extent these developments are driven by land reclamations or other human interference. Based on long-term observations that span the time of morphological adaptation to tidal flat reclamations, here we explore if the evolution of real-world tidal systems agrees with the theoretical frameworks describing the evolutionary trajectory towards morphological equilibrium.

The aim of this paper is to understand how loss of intertidal area by land reclamations influences estuarine morphodynamic development. We focus on the Ems estuary, located on the border between the Netherlands and Germany and part of the Wadden Sea tidal lagoon, which represents a heavily human-modified tidal system. The most important anthropogenic pressures in the Ems include large-scale tidal flat reclamation of storm-surge formed embayments, which started in the beginning of the 16^{th} century. This was followed by fairway re-alignment, deepening, and maintenance dredging since the 20^{th} century (Van Maren et al., 2016). First, we reconstruct the land reclamation history (Section 3.1). Second, we reconstruct and analyze the historical and contemporary development of the estuarine channels and tidal flats over the past 500 years (Section 3.2). A multichannel system with distinct ebb- and flood channels (Van Veen et al., 2005) in the estuary has degenerated into a single channel in the 20^{th} century (Gerritsen, 1952), which is still poorly understood. Two hypotheses exist explaining these channel pattern changes: (1) channel system instability due to fairway deepening and related sediment disposal (Van Veen et al., 2005; Van Veen, 1950), and (2) tidal prism decrease as a result of intertidal storage loss due to land reclamation (Gerritsen, 1952). We discuss the controls of land reclamation versus channel deepening on the observed channel pattern changes and interpret these findings using tidal asymmetry-based estuarine equilibrium relationships (Section 4).

2 Material and Methods

Reclaimed land surface area was reconstructed from several data sources described below, and archived in Schrijvershof (2024). The main sources for the reconstructions on the Dutch shore of the Ems estuary are geospatial datasets with the location of historical embankments[1] and the National Historical Culture registry[2]. This information was supplemented with information from maps presented by Knottnerus (2013a) and Van Maren et al. (2016), to determine the year in which a reclamation was completed. Digital elevation models (DEMs) of the surface topography, aerial imagery (allotment pattern), and palaeogeographical reconstructions (P. C. Vos & Knol, 2015, 2013) were used to detail the maximum extent of storm-surge-formed bays, to include the oldest (poorly-documented)

[1] https://geoportaal.provinciegroningen.nl/portal/apps/experiencebuilder/experience/?id=9e93c75c4e5e47a584829e1deb0ad5f6

[2] https://nationaalgeoregister.nl/geonetwork/srv/dut/catalog.search#/metadata/9a9cef3a-2dfc-4aa8-b248-f73f4064d7ad

reclaimed lands. The maximum extent of the Dollard Bay, in particular, increased through this approach, leading to a reclamation reconstruction that largely agrees with the map presented by Knottnerus (2013a). The reclamation history on the German part of the Ems estuary is digitized from maps presented by Homeier (1962) and Homeier et al. (1969)[3]. The reclamation history of Sielmönken bay could not be reconstructed but the approximate maximum extent of the embayment is derived from DEMs and aerial imagery. The lands reclaimed along the tidal river (landwards of the port of Emden) are not included in the land reclamation database (Schrijvershof, 2024) because the focus of this paper is on the mouth and transitional regions of the Ems estuary.

The morphological evolution of the Ems estuary is reconstructed for the period with intense anthropogenic interventions since the 16^{th} century. A unique long-term record of geospatial datasets is compiled that almost completely covers this time-period (Table 1). The datasets were collected from published literature (Lang, 1954; Homeier, 1962; Gerritsen, 1952; Stratingh & Venema, 1855), published data sources (H. Pierik, 2019; Sievers et al., 2021), or collected from national archives, and were provided in digitized format (Herrling & Niemeyer, 2007, 2008; De Jong, 2006) or, otherwise, digitized using GIS software. The recent gridded topo-bathymetrical datasets (1985-2020) are publicly available at Rijkswaterstaat[4] and WSA Emden[5]. The datasets can be divided in three categories: (1) historical reconstructions of channel and tidal flat planform, based on a large variety of written and illustrated sources, but interpreted and compiled in the 20^{th} century, (2) digitized nautical charts originally collected in hydrographic surveys for military and water way organizations, and (3) recent (1937, 1985-2020) full coverage digital elevation models (DEM) collected through (echo) sounding observations. All geospatial datasets were provided or converted in a digitized format (Table 1) and published with this paper (Schrijvershof, 2024). The three types of datasets provide different kind of geospatial information. The historical reconstructions only reveal the geographical location of the Mean Low Water line (MLW), Mean High Water line (MHW) and fixed bank lines; the nautical charts provide a DEM of the subtidal (below MLW) domain; and the recent sounding observations provide a full DEM of the subtidal, intertidal and supratidal domain. Contour lines of MLW and MHW are derived from the recent DEMs using an along-estuary averaged value for MLW (NAP -1.50 m) and MHW (NAP +1.30 NAP), following Arcadis (2011). The spatial extent of the geospatial datasets varies and do not all cover the full extent of the estuary. Datasets with incomplete coverage are not used for all analyses. The accuracy and precision of the geospatial information are lower for older datasets than for more recent datasets. The historical reconstructions of pre-19^{th}-century morphology (made in the 20^{th} century), in particular, are constructed with considerable interpretation of the original authors who drafted the maps. The inaccuracies of older maps therefore introduce uncertainty in the metrics we develop as part of our morphological analysis. We minimize the impact of such uncertainties by collecting data from multiple sources and authors, and by focusing on morphological trends based on a wide range of independent datasets.

We identify and quantify the main morphological changes in the estuary over the past 500 years. Subtidal surface area (A_c) and intertidal surface area (A_s) are derived from enclosed areas formed by MLW, MHW, and fixed bank lines. These surface area metrics are, due to data availability, quantified for a region that includes the Dollard Bay and the central estuary, but excludes the mouth zone with the tidal inlets (see Figure S4 in Supporting Information S1). Channel geometry metrics (area, depth, volume) are

[3] https://www.nlwkn.niedersachsen.de/startseite/hochwasser_kustenschutz/kustenschutz/ausgewahlte_projekte/kustenschutz_projekt_leybucht/kuestenschutz-projekt-leybucht-43552.html

[4] https://www.rijkswaterstaat.nl/formulieren/contactformulier-servicedesk-data

[5] https://www.wsa-ems-nordsee.wsv.de/Webs/WSA/Ems-Nordsee/DE/00_Startseite/startseite_node.html

derived as spatial mean values for areas defined in the outer, central, and inner estuary and along a defined cross-section covering the central-estuary channels (Figure 1).

Contextual background information on the historic landscape developments and the most important human-landscape interactions in the Ems estuary is provided in Supporting Information S1. Palaeogeopgraphical reconstructions, presented by P. Vos et al. (2020); P. C. Vos and Knol (2015, 2013), were modified to show and describe the inherited geological setting and Holocene evolution of the Ems estuary region (Section S1.1 in Supporting Information S1). The historic evolution is particularly relevant to understand the formation of the storm surge-formed embayments that were reclaimed (Section S1.2 in Supporting Information S1). The 20th-century human-landscape interactions, particularly relevant for the recent observed morphological developments, include channel dredging, port construction, and channel-realignments. An overview of these anthropogenic works is presented in Section S1.3 in Supporting Information S1.

3 Results

3.1 Land reclamation reconstruction

In the Ems estuary region land reclamation works started probably in the 11th century (Homeier et al., 1969; Behre, 1999). The former "Sielmönken bay" (Figure 1), a former sea ingression that reached its largest extent between 800 and 950 A.D., was already completely reclaimed in the 13th century. The Fivel bay (Figure 1) started to silt-up prior to human settlement because outflow of the Fivel river was hampered by expanding shore ridges (P. Vos & van Kesteren, 2000). The process was accelerated because, from the 12th century onwards, embankments were constructed and the flow from the Fivel river was redirected to artificial tidal shipping canals (Knottnerus, 2013b). Reclamation of the Fivel bay continued untill the 15th century, after which the seaward shoreline extension continued in the 19th century with improved reclamation techniques. The most recent coastal reclamation was the construction of a large seaport in the 1970's. The Ley bay reclamations started in the 15th century and continued until the 20th century (Figure 1). The Dollard bay reclamations are the largest reclamation works in the estuary (Figure 1), starting at the beginning of the 16th century (Figure 1) and continuing far into the 20th century. The land surface elevations of the Dollard reclamations clearly show the decrease in land surface level with reclamation age (Figure 1), because older reclaimed areas subsided more due to peat oxidation and compaction. The Dollard bay was never completely reclaimed (≈20% remained) and is nowadays highly valued and protected as a unique tidal flat and salt marsh landscape. Reclamations near the port city of Emden were executed to relocate the city harbor towards the river (Figure 1), after it lost its access due to a meander bend cut-off (see Section S1.2 in Supporting Information S1). In an effort to narrow and deepen the Emden access fairway, the tidal flats west of Emden were reclaimed as well. The most recent reclaimed land in the inland part of the estuary is the construction of the "Rysumer Nacken" (Figure 1). The 1933 completion of a bended longitudinal training dam, constructed to redirect the navigational channel[6], was followed-up by landfill deposits on the sheltered tidal flats with dredged material[7].

The total cumulative amount of land surface reclaimed in the region of the Ems estuary since the start of reclamation works (12th century) is approximately 700 km^2 (Figure 2). The Dollard Bay reclamations constitute half (≈360 km^2) of the total reclaimed land. The reclamation rate in Dollard Bay decreased halfway through the 19th century, while the Fivel Bay and Ley Bay reclamations accelerated slightly around this time. Including all reclamation regions, there has been a continuous reclamation rate of ≈100

[6] `https://delibra.bg.polsl.pl/Content/22564/heft53_54.pdf`
[7] `https://de.wikipedia.org/wiki/Rysumer_Nacken`

248 km^2 per century since the Dollard reclamations started in the beginning of the 16$^{\text{th}}$ cen-
249 tury. The extent of the Ems estuary was largest after the formation of Dollard Bay in
250 1509 (≈1750 km^2) and decreased due to the land reclamation works to a present-day size
251 of ≈1200 km^2. The reclamation works reshaped the estuary outline and decreased $\approx \frac{1}{3}$
252 of the total basin extent. The Dollard Bay reclamations make up 65% of this reduction.

253 ### 3.2 Morphological reconstruction

254 ***Channel-flat configuration***

255 The 16$^{\text{th}}$-century morphology consisted of multiple tidal channels and tidal flats
256 consisting of fringing flats and mid-channel bars, or shoals (Figure 3a). A double inlet
257 system flanking the barrier island Borkum, connected the estuary and the North Sea.
258 The two inlets had approximate equal planform sizes, yet the western inlet was more ef-
259 ficiently connected to the central-estuary (see Figure 1 for demarcation) channels. The
260 eastern inlet also drained the tidal volume of the Ley Bay, most of which was not yet
261 reclaimed in the 16$^{\text{th}}$ century (Figure 1). The central part of the estuary is bisected by
262 a western and an eastern channel, hereafter referred to as the western channel and east-
263 ern channel. In the 16$^{\text{th}}$-century the western channel dominates over the eastern chan-
264 nel and connects via a meander bend to the western inlet in the outer estuary. In the
265 18$^{\text{th}}$ century (Figure 3b) the orientation of the channel connecting the eastern tidal in-
266 let with the central-estuary channels changes while shrinking in size. A mid-channel shoal
267 develops in the outer estuary western inlet. The central-estuary shoal complex migrates
268 westward, resulting in an increase of the size of the eastern channel at the expense of the
269 western channel. Despite this, the western channel remains to be the main channel. Sub-
270 tidal bathymetries, available from the start of the 19$^{\text{th}}$ century (Figure 3c, Figure S5 in
271 Supporting Information S1), reveal the depths of the main estuarine channels. The main
272 channel route starts from the western inlet via the western channel into Dollard Bay. The
273 sinusoidal meandering pattern with mid-channel shoals confirms the multichannel ebb-
274 flood pattern reported by Van Veen (1950) and Gerritsen (1952).

275 The connection of the eastern inlet to the central-estuary channels degenerated from
276 a well-connected channel in the 16$^{\text{th}}$ century into a tidal divide in the 18$^{\text{th}}$ century to
277 beginning of the 19$^{\text{th}}$ century (see Figure 3b, c). The main tidal channels are filling in
278 with sediments in the 20$^{\text{th}}$ century (compare Figure 3c with d and e) while degenera-
279 tion of the former connection with the eastern tidal inlet progresses until it is completely
280 disconnected in the 21$^{\text{th}}$ century (Figure 3f). The tidal shoal complex in the central-estuary
281 zone becomes larger and migrates further westward. At the same time, the western chan-
282 nel degenerates (becoming shallower and narrower) while the eastern channel deepens
283 and widens. During the 20$^{\text{th}}$ century, the meander bend connecting the outer estuary
284 channels with the central-estuary channels (see Figure 1) is straightened, resulting in a
285 reduction of channel sinuosity (H. J. Pierik et al., 2022). The southern section of the central-
286 estuary eastern channel moves westward (Figure 3d), presumably forced by the construc-
287 tion of a longitudinal training wall (Figure 1). The present-day situation shows that the
288 western channel has now degenerated into a minor channel (Figure 3f).

289 The land reclamation works and the channel and tidal flat pattern developments
290 illustrated in Figure 3 influence the areas occupied by tidal channels (A_c) and tidal flats
291 (A_s). Up to the end of the 19$^{\text{th}}$ century, A_s decreased (Figure 4), which is a result of land
292 reclamation in Dollard Bay (Figure S4 in Supporting Information S1). Since the begin-
293 ning of the 20$^{\text{th}}$ century the tidal flat surface area gradually increased because of expan-
294 sion of the central-estuary shoal complex, and degeneration of the eastern inlet connec-
295 tion to the central-estuary channels (Figure S4 in Supporting Information S1). A_c is more
296 variable over the reconstructed time period but shows, in general, a decreasing trend.
297 This decrease is due to the loss of tidal channels in the progressively reclaimed Dollard
298 Bay (up till the 20$^{\text{th}}$ century), and the central-estuary channel transition from a dou-

ble to single channel system. The estuary-scale A_s/A_c ratio decreases up to the beginning of the 20th century, and since then increases again (Figure 4). The decrease in A_s/A_c is mostly attributed to a loss in A_s (due to land reclamations works) whereas the increase in A_s/A_c is mostly attributed to a loss of subtidal area A_c (resulting from subtidal infilling).

Channel dimensions

Metrics of channel geometry, derived since the first available subtidal bathymetry in 1833 show that in the period 1833 - 1900 the total central-estuary channel area decreased (Figure 5a). The channels became shallower (Figure 5b), and as a combined result, the channel volume decreased (Figure 5c). After 1900, the subtidal area further decreased (Figure 5a and Figure 4). The remaining single channel, however, deepened (Figure 5b) and, as a result, the subtidal volume of the central-estuary channels remained mostly constant during the 20th century (Figure 5c). This deepening is partly natural, but since the 1970's deepening accelerated by increasing maintenance dredging for navigation purposes (Figure S3 in Supporting Information S1). In the inner estuary, the subtidal volume has been nearly constant since 1888, because a decrease of subtidal area was compensated for by an increase in channel depth (Figure 5b). The subtidal volume of the outer estuary inlet increased (Figure 5c) and expanded (Figure 5a), presumably because the western inlet accommodated the tidal volume exchange of the disconnected eastern inlet. The depth of the outer estuary western inlet first decreased and later increased, which may be the result of the dynamic character of the inlets, influenced by tidal discharge, and wave-driven along-shore (eastwards) sediment transport.

Cross-sectional geometry metrics (see Figure 1 for the location of cross-section A-A') show that the width (W_{cs}) of the central-estuary channels (Figure 6a) has been changing very consistently since the oldest available historical reconstruction from 1580. The western channel width decreased steadily with ≈300-400 m/century up to 1900, after which the channel width abruptly narrowed. In the past decades the rate of change decreased again, but channel width continues to decrease up till present. The eastern channel width steadily increased with ≈ 250 m/century over the reconstructed period. The cross-sectional deepest point (Figure 6b) and cross-sectional area (Figure 6c) both show consistent trends of channel shoaling in the western channel and channel deepening in the eastern channel since the beginning of the 19th century. The change in the deepest point in the cross-section appears, similarly to channel width, to accelerate in the 20th century.

4 Discussion

4.1 Adaptation timescales to land reclamation

The centennial-scale morphological reconstructions of the Ems estuary show that since the beginning of the land reclamation works in the 16th century the morphology of the estuary has been changing. The loss of estuarine tidal flats resulted in pronounced infilling of tidal channels. The channels and tidal flats in the central area and Dollard Bay clearly show this morphological response, despite 20th-century intensified channel dredging favoring an increase in subtidal volume. The channel and tidal flat adaptation demonstrates that the response time of estuaries to large-scale ($\frac{1}{3}$ of basin extent) and continued land reclamation is in the order of centuries. This response time to human interventions depends on the processes driving the change, the size of the system, and the magnitude of the intervention (van Maren, Colina Alonso, et al., 2023) as well as accommodation space and sediment supply (Beets et al., 1992).

Intertidal storage volume decreased due to the reclamation of tidal flats. The decrease will lead to a smaller tidal prism conveyed through the tidal channels (Speer & Aubrey, 1985; Friedrichs & Aubrey, 1988), and channel infilling because the channel di-

mensions correspond to a pre-reclamation tidal volume exchange (Dronkers, 2016). In short tidal basins, the basin geometry change (Dronkers, 1986; Friedrichs & Aubrey, 1988; Ridderinkhof et al., 2014) and a reduction in friction (Fortunato & Oliveira, 2005) increase tidal asymmetry-driven import of sediment. In the Ems estuary, the main source of sediment is of marine origin (the Wadden Sea and/or North Sea), and the sediment load carried by the Ems river is small (Van Maren, van Kessel, et al., 2015). With abundant supply of sand from the adjacent shallow sandy seabed (van der Molen & de Swart, 2001) and of mud supplied by the nearby Meuse and Rhine rivers, the tidal embayments along the Dutch coast filled up rapidly during the Holocene (van der Spek, 1994; de Haas et al., 2018). Despite the abundant sediment supply, the Ems Estuary required centuries to adapt to human interventions.

Globally, dredging activities have accelerated in the past century (Talke & Jay, 2020). The hydro-morphodynamic conditions of estuaries and tidal basins in the pre-dredged era are often taken as a reference to study the impact of channel deepening (Ralston et al., 2019; Bao et al., 2022; Siemes et al., 2023), maintenance dredging and disposal (Vellinga et al., 2014; Jeuken & Wang, 2010; van Dijk et al., 2021), or a combination (Van Maren, van Kessel, et al., 2015). Our results demonstrate that estuaries along which land was reclaimed are unlikely to be in morphological equilibrium. Pre-19$^{\text{th}}$-century land reclamation may still impact the present-day morphodynamic evolution, which needs to be taken into account when differentiating between natural controls and recent human modifications (Monge-Ganuzas et al., 2013; Dai et al., 2016; Zhu et al., 2019). The morphodynamic impact of future newly proposed interventions (e.g., Cox et al., 2006; Weisscher et al., 2022) should carefully embed the lagging effects of a still adapting morphology.

4.2 Tidal asymmetry and system resilience

The loss of intertidal area due to tidal flat reclamation distorts the estuary-scale configuration of channels and tidal flats, which is quantified with a ratio A_s/A_c. Land reclamations resulted in a decrease in A_s/A_c over several centuries, but the ratio increases again after 1937 (Figure 4). The reason for this change is stabilization of the tidal flat area (no more reclamations) while the subtidal area continued to decrease due to infilling in response to a smaller tidal prism. The reconstructed channel-flat ratio in the Ems estuary provides a unique long-term record, which allows testing stability theory.

Tidal inlet stability theory typically relates a metric for residual sediment transport (the type and degree of tidal asymmetry) to a metric representing the relative importance of flow over flats and channels. The type of tidal asymmetry is the result of a competition between frictional interaction between the tide and the channel bed (captured in the tidal amplitude over channel depth ratio, a/h) and the relative intertidal water storage capacity (captured in the intertidal volume over channel volume ratio, V_s/V_c) (e.g., Friedrichs & Aubrey, 1988; Z. Wang et al., 1999; Dronkers, 2016). Various types of tidal asymmetry-based stability relationships have been developed, which are quite consistent, as demonstrated by Zhou et al. (2018). Comparisons between the stability relationships and field-based conditions of real-world systems (Dronkers, 2016; Zhou et al., 2018), however, shows considerable discrepancy. The discrepancy is due to the assumptions that inevitably have to be made to facilitate the analytical solutions (for example, simplifications of the cross-sectional geometry) and uncertainties in real-world observations (Zhou et al., 2018).

To apply existing equilibrium realtionships to the Ems Estuary, the subtidal and intertidal surface areas are converted to subtidal and intertidal volumes, following Zhou et al. (2018) and assuming a rectangular cross-sectional geometry:

$$V_s = 2a(S_{HW} - S_{LW}) \tag{1}$$

$$V_c = h(S_{LW}) \tag{2}$$

Here, S_{HW} and S_{LW} are the surface area at high water and low water, respectively. The surface area at low water is equal to the reconstructed subtidal area ($S_{LW} = A_s$) and the surface area at high water results from addition of the subtidal and intertidal areas ($S_{HW} = A_s + A_c$). The parameter a is the tidal amplitude at the mouth of the estuary (equal to 1.2 m; see Herrling and Niemeyer (2007)) and assumed constant for the reconstructed period (H. J. Pierik et al., 2022). The mean water depth h is taken as the average channel depth (following Zhou et al. (2018)), and can only be computed since the availability of subtidal DEMs (beginning of the 19$^{\text{th}}$ century). Linear interpolation and extrapolation provide the values of h at the moments the channel-flat configuration is known (Figure 4). The evolutionary trajectory of the reconstructed Ems estuary (Figure 7) in the stability diagram shows that up till the beginning of the 20$^{\text{th}}$ century, the system evolved towards a more flood dominant regime (increasing a/h), but became more ebb dominant since then (decreasing a/h and increasing V_s/V_c). Such an evolutionary trajectory from an increasingly flood dominant system to ebb-dominant conditions agrees with the theoretical trajectory of an estuarine system responding to land reclamation (Dronkers, 2016). The agreement between the observed and theoretical trajectories suggests a certain resilience of the morphodynamic system, because there is system tendency towards a morphodynamic equilibrium state. A delta system is defined as resilient when it has the capacity to recover from an extreme forcing at one of its boundaries and is largely self-sustaining (i.e., not in need of high maintenance) (Hoitink et al., 2020). In this case, the anthropologically disturbed channel-flat configuration is the forcing and the morphodynamic system response through tidal asymmetry-driven import of sediment restores this configuration.

4.3 Controls on channel-flat dynamics

The channel-flat pattern in the Ems estuary transitioned from a double-inlet multichannel system with mutually evasive ebb- and flood channels separated by shoals, towards a channel system consisting of a single inlet with a main channel and less pronounced ebb- and flood channels. The degeneration of the connection with the eastern Ems inlet and the central-estuary channel system change are the most pronounced channel pattern developments. These channel dynamics can be observed since the 16$^{\text{th}}$ century (Figure 3) untill present, indicating a permanent channel pattern change with no tendency of re-establishment of the multi-channel system. Considering that these developments started in the 16$^{\text{th}}$ century, the loss of the characteristic multichannel pattern is not caused by channel re-alignment and dredging works in the 19$^{\text{th}}$ and 20$^{\text{th}}$ centuries (Van Veen, 1950; Van Veen et al., 2005). The past decadal developments of channel geometry do show a clear signature of dredging activity (Figure 5, Figure 6) but these changes are superimposed on the long-term system-scale response to the loss of intertidal areas (Figure 4, Figure 7). The most likely trigger for the channel pattern change is thus the loss of intertidal areas landward of the central-estuary channels and the resulting decrease of the tidal volume exchange (Gerritsen, 1952), predominantly caused by reclamation of Dollard Bay.

The loss of a naturally stable multichannel ebb- and flood system has previously been related to dredging and disposal activities (Monge-Ganuzas et al., 2013), because a change in flow and sediment distribution can lead to bifurcation instability and subsequent channel degeneration (avulsion) (Z. B. Wang & Winterwerp, 2001; Jeuken & Wang, 2010). Here, we present a system in which the degeneration of the multichannel system is not primarily caused by dredging and disposal activities but by land reclamation, although dredging works may have accelerated the response to land reclamations. This points to a relation between the tidal prism and the number of channels in an estuary or tidal basin.

The cross-sectional area (A) of a tidal inlet is linearly correlated to the tidal prism (P) (O'Brien & P., 1931; Jarrett, 1976). This well-known tidal prism-area (P-A) relationship is argued to be applicable along the entire length of the tidal channel (D'Alpaos et al., 2010), although it seems to have upper and lower limits (a. Hibma et al., 2004). In the Western Scheldt estuary, a channel will bifurcate into more channels if the cross-sectional area exceeds 25.000 - 30.000 m^2 (Allersma, 1992; Voorsmit, 2006). Interestingly, the total cross-sectional area of the central-estuary channels in the Ems estuary equaled this critical value in the 19^{th} century (Figure 6c), shortly after which the multichannel system degenerated. This supports that the loss of the multichannel system results from a reduction in cross-sectional area, which in turn is the result of channel infilling due to lower tidal flow velocities. The range in the critical cross-sectional area found in the Western Scheldt is, however, not universally constant, but depends on the size of the system and type of sediment in the estuary (Allersma, 1994). The number of channels is limited by the width to depth ratio of the estuary cross-section, with an increasing number of channels with increasing estuary width (Stive & Wang, 2003). The development of quantitative relationships between the number of tidal channels and the tidal prism, the cross-sectional area, and the width to depth ratio of the estuary is a contemporary challenge that is crucial in making future predictions for estuarine morphology.

5 Conclusion

The land reclamation history and the morphodynamic evolution of the Ems estuary were reconstructed since the beginning of 16^{th} century. The reconstructions show that the morphodynamic evolution of the Ems estuary is heavily influenced by land reclamation works, particularly by those carried out in the Dollard Bay. The loss of intertidal storage volume as a result of tidal flat reclamation reduces the tidal prism, which leads to subtidal infilling. Interpretation of the long-term change in tidal channels and flats shows that the system-scale morphodynamic adaptation is controlled by the effects of land reclamation. Channel deepening and maintenance dredging in the 20^{th} century cumulatively impacted the system, while still adapting to the land reclamation works. The disconnection of a tidal inlet to the main estuarine system, and the transition from a multichannel-shoal complex towards a single channel configuration with fringing flats, is shown to be primarily forced by the effects of land reclamation. Dredging works and channel re-alignment have likely accelerated these developments. The centennial-scale historical analysis shows that estuarine systems follow the evolutionary trajectory predicted by tidal asymmetry-based stability theory as they move toward a new equilibrium configuration with modified tidal flats and channels. The channel pattern transition - from a multichannel single channel system - is found to be related to the changes in tidal prism and the width to depth ratio of the estuary.

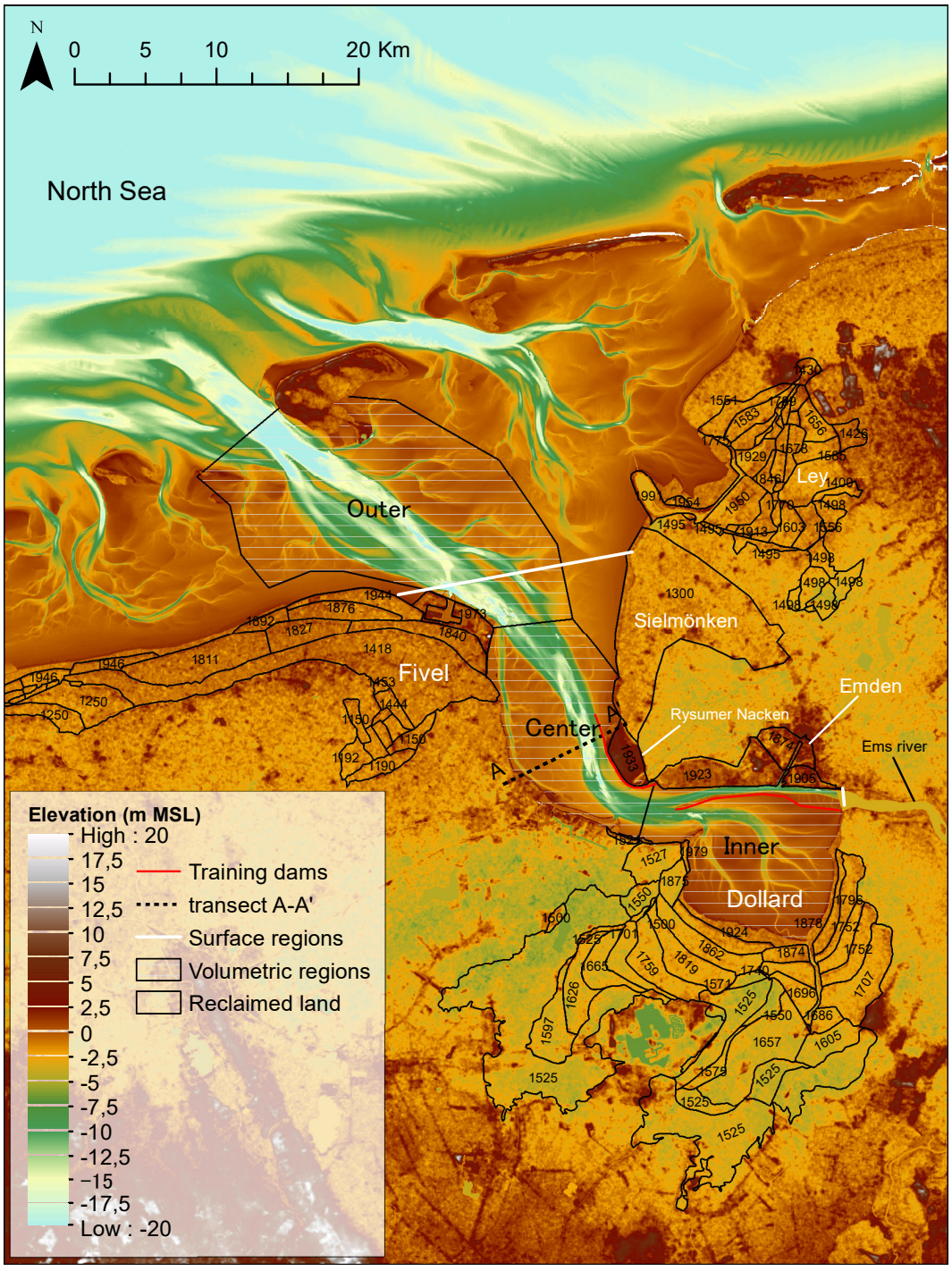

Figure 1. Land surface reclaimed in the region of the Ems estuary, with the year of completion indicated in the reclaimed area. The background color-scale visualizes the present-day topo-bathymetric Digital Elevation Model, compiled from multiple sources (see Open Research section, Section 5)

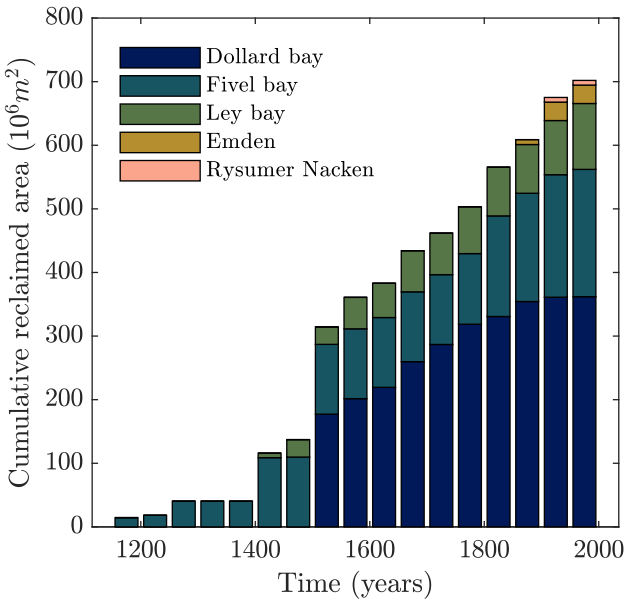

Figure 2. Cumulative area reclaimed since the 12$^{\text{th}}$ century, summed over half-century periods and subdivided for each defined land reclamation region.

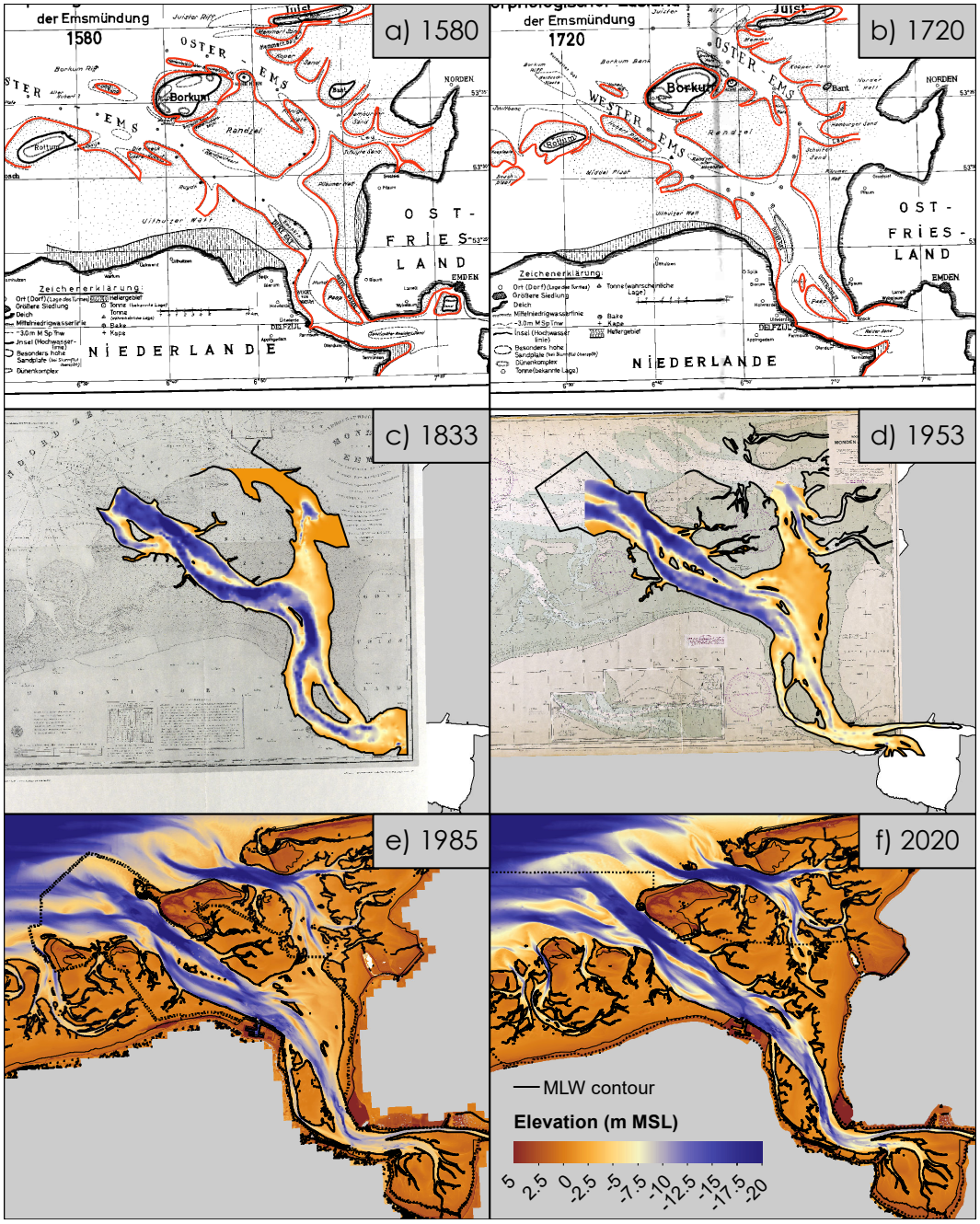

Figure 3. Centennial morphological evolution of the Ems estuary, based on: historical reconstructions of Lang (1954) (a, b); reconstructed subtidal bathymetry from H. J. Pierik et al. (2022); H. Pierik (2019) (c, d); and compiled datasets of echo sounding observations from the years 1985 and 1996 (e) and the years 2016 and 2020 (f). The Mean Low Water line is shown in red (a, b) and black (c, d, e, f). On the two most recent maps (e, f) the present-day outline of the estuary is shown and the dotted lines indicate the extent of the Rijkswaterstaat datasets.

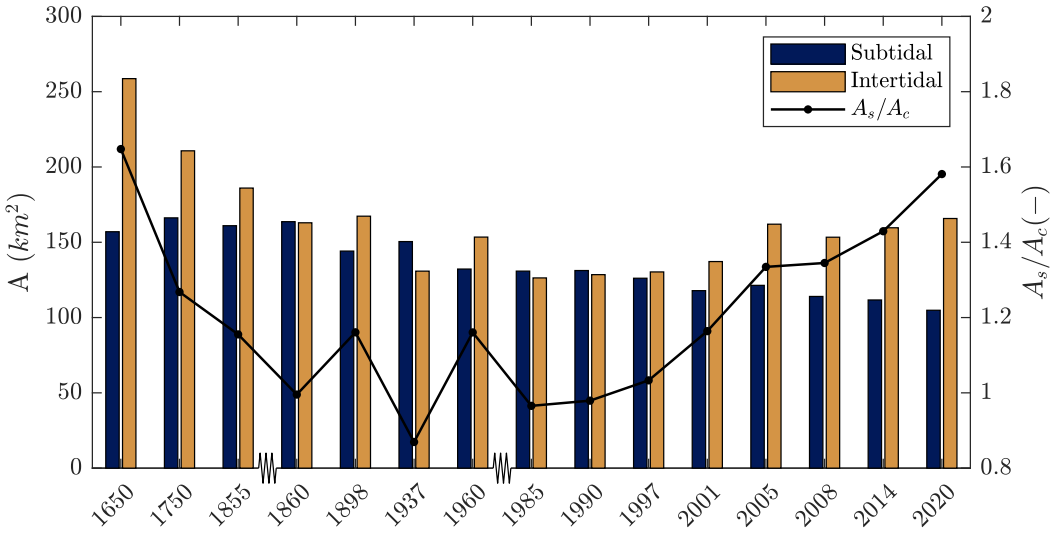

Figure 4. Subtidal and intertidal surface area (A) and subtidal to intertidal surface area ratio (A_s/A_c) in the estuarine zone, excluding the mouth zone (see Figure 1 for the demarcation of the estuarine zone). The zigzags on the x-axis indicate a time-scaling discontinuity.

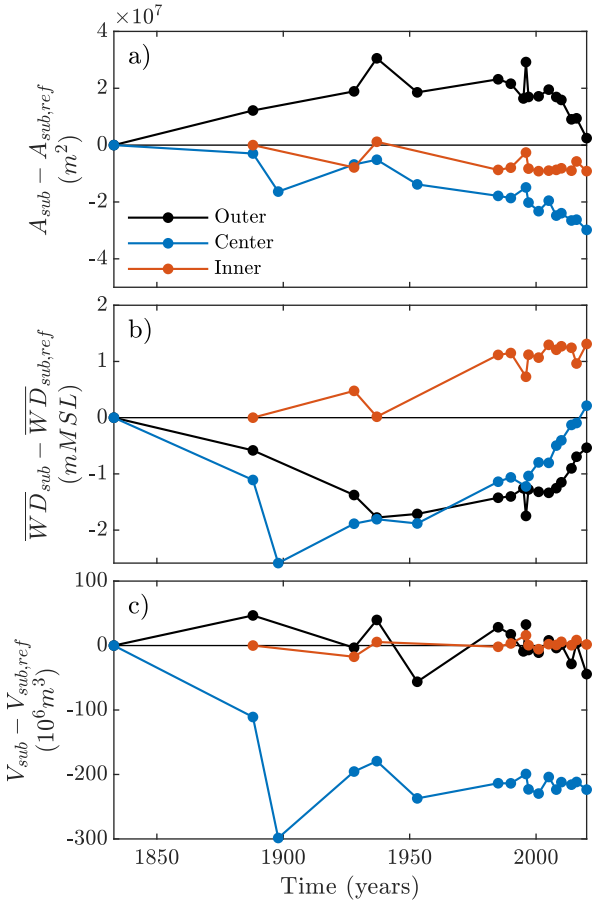

Figure 5. Relative change of the subtidal (below Mean Low Water) area A_{sub} (a), mean water depth $\overline{WD}_{sub}$ (b, with negative values implying shallower channels) and volume V_{sub}(c) with respect to the same properties derived from the first available subtidal bathymetry (1833 or 1888), depending on the region.

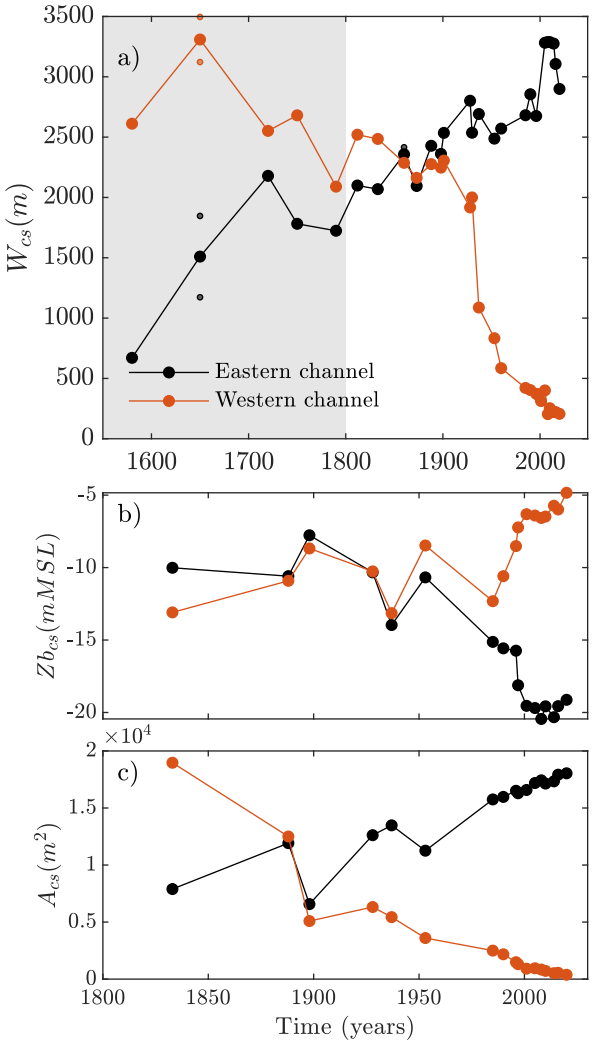

Figure 6. Channel width W_{cs} (a), deepest point Zb_{cs} (b), and cross-sectional volume V_{cs} (c) along the cross-section A-A' in Figure 1. Note that the channel geometry metrics are shown for time periods with data availability, leading to a longer time span in panel a (indicated by a gray patch) than in panels b and c. Channel width in panel shows averaged values for years with multiple sources available.

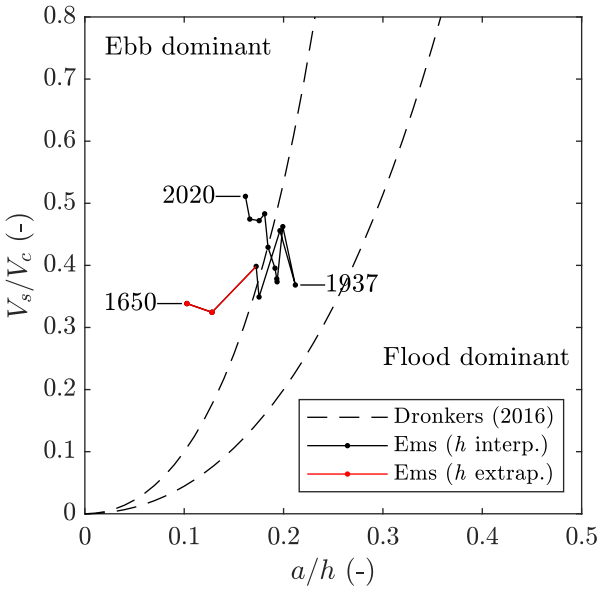

Figure 7. Tidal asymmetry based on the stability diagram in Zhou et al. (2018). For the Ems estuary data, V_s/V_c is derived by applying equations 1 and 2 on the surface areas from the morphological reconstructions, the tidal amplitude a is assumed constant at 1.2 m, and the mean water depth h is derived from linear interpolation and extrapolation (red data points) on the subtidal DEMs. The stability curves represent the analytical expressions derived by Dronkers (2016) with $\gamma = [1,2]$.

Table 1. Overview of the type and sources of the geospatial datasets gathered and digitized for this study.

Year	Format & resolution	Original source	Digitized source
1580	MLW contours	Hist. reconstruction (Lang, 1954)	This article
1650	MLW contours	Hist. reconstruction (Lang, 1954)	This article
1650	MLW, MHW and supratidal contours	Hist. reconstruction (Homeier, 1962)	Herrling and Niemeyer (2007)
1720	MLW contours	Hist. reconstruction (Lang, 1954)	This article
1750	MLW, MHW and supratidal contours	Hist. reconstruction (Homeier, 1962)	Herrling and Niemeyer (2007)
1790	MLW contours	Hist. reconstruction (Lang, 1954)	This article
1812	LLW contours	Hist. reconstruction (Gerritsen, 1952)	This article
1833	Gridded (100x100)	Nautical chart Dutch dep. of defense	H. J. Pierik et al. (2022); H. Pierik (2019)
1855	MLW, MHW and supratidal contours	Hist. reconstruction (Stratingh & Venema, 1855; Gerritsen, 1952)	De Jong (2006)
1860	MLW contours	Hist. reconstruction (Lang, 1954)	This article
1860	MLW, MHW and supratidal contours	Hist. reconstructions (Homeier, 1962; Gerritsen, 1952)	Herrling and Niemeyer (2007)
1873	MLW contours	Hist. reconstruction (Gerritsen, 1952)	This article
1888	Gridded (100x100)	Nautical chart Dutch dep. of defense, Hist. reconstruction Relative change of the subtidal (Homeier, 1962)	H. J. Pierik et al. (2022); H. Pierik (2019)
1898	Gridded (20x20)	Nautical charts Ems Mündung (1:50000) & Die Ems Von Delfzijl Bis Pogum (1:25000) von Reichs Marine Amt	This article
1901	MLW contours	Hist. reconstruction Gerritsen (1952)	This article
1928	Gridded (100x100)	Nautical chart Dutch dep. of defense	H. J. Pierik et al. (2022); H. Pierik (2019)
1930	MLW contours	Hist. reconstruction (Lang, 1954)	This article
1937	Gridded (5x5)	Depth soundings (German marine, RWS, Waterway agency Emden & Meppen)	Herrling and Niemeyer (2008)
1953	Gridded (100x100)	Nautical chart Dutch dep. of defense	H. J. Pierik et al. (2022); H. Pierik (2019)
1960	MLW, MHW and supratidal contours	Hist. reconstructions (Homeier, 1962; Gerritsen, 1952)	Herrling and Niemeyer (2007)
1985	Gridded (20x20)	Echo soundings	Rijkswaterstaat
1990	Gridded (20x20)	Echo soundings	Rijkswaterstaat
1996	Gridded (10x10)	Echo soundings	Sievers et al. (2021)
1997	Gridded (20x20)	Echo soundings	Rijkswaterstaat
2001	Gridded (20x20)	Echo soundings	Rijkswaterstaat
2005	Gridded (20x20)	Echo soundings	Rijkswaterstaat
2008	Gridded (20x20)	Echo soundings	Rijkswaterstaat
2010	Gridded (25x25)	Echo soundings	WSA Emden
2014	Gridded (20x20)	Echo soundings	Rijkswaterstaat
2016	Gridded (10x10)	Echo soundings	Sievers et al. (2021)
2020	Gridded (20x20)	Echo soundings	Rijkswaterstaat

Open Research Section

Figure 1 is compiled from various sources of topo-bathymetric data to construct a full coverage DEM, all sources are publicibly available. The data sources include the land surface topography at 25 m resolution provided by Copernicus (EU-DEM - version 1.1, Apr. 2016; `https://doi.org/10.5270/ESA-c5d3d65`), subaqueous bathymetry of the North Sea at ≈90 m resolution provided by the European Marine Observation and Data Network (EMODnet - `https://emodnet.ec.europa.eu/en/bathymetry`) and the coastal bathymetry which was requested through the servicedesk data of Rijkswaterstaat (`https://www.rijkswaterstaat.nl/formulieren/contactformulier-servicedesk-data`).

The main sources for the reconstruction of the land reclamation history are geospatial datasets with the location of historical embankments (`https://geoportaal.provinciegroningen.nl/portal/apps/experiencebuilder/experience/?id=9e93c75c4e5e47a584829e1deb0ad5f6`) and the National Historical Culture registry (`https://nationaalgeoregister.nl/geonetwork/srv/dut/catalog.search#/metadata/9a9cef3a-2dfc-4aa8-b248-f73f4064d7ad`). The

land reclamations reconstructions are published (Schrijvershof, 2024) and available at 4TU.ResearchData (https://data.4tu.nl/datasets/78ac0cf9-e9f7-47c7-8c4e-93f7fb2c633e/1).

The morphological reconstructions are based on a large number of historical maps, reconstructions and data sources, all listed in Table 1. All maps that were georeferenced and digitized (MLW, MHW, and supratidal contours) in this study (Lang, 1954; Gerritsen, 1952) and the the maps of Homeier (1962) are included in Schrijvershof (2024). The digitized reconstructions made by Herrling and Niemeyer (2007) from the maps of Homeier (1962) were provided by the Niedersächsischer Landesbetrieb für Wasserwirtschaft, Küsten-und Natur- schutz (NLWKN) and can be contacted for the data. The gridded (subtidal) bathymetry datasets are available through the references included in Table 1 and therefore not included in Schrijvershof (2024).

Acknowledgments

This work was funded by the Netherlands Organisation for Scientific Research (NWO) within Vici project "Deltas out of shape: regime changes of sediment dynamics in tide-influenced deltas" (Grant NWO-TTW 17062) and Deltares Research Funds.

This study is based on and relied on an enormous quantity of historical data sources compiled from old literature, that is often not well-disclosed. We want to thank all involved that supported the collection of the required datasets that made this study possible. In particular the colleagues from Niedersächsischer Landesbetrieb für Wasserwirtschaft, Küsten-und Natur- schutz (NLWKN) for providing the digitized reconstruction of (Homeier, 1962) and our colleague Joris Beemster who generously helped on gathering and digitizing the 1898 Nautical Charts from the Reichs Marine Amt.

References

Alebregtse, N. C. (2015). *Modeling the Hydrodynamics in Tidal Networks* (Unpublished doctoral dissertation). Utrecht University, Utrecht. (ISBN: 9789462992597)

Allersma, E. (1992). *Studie inrichting Oostelijk deel Westerschelde. Analyse van het fysische systeem* (Tech. Rep.).

Allersma, E. (1994). *Geulen in estuaria: 1-D modellering van evenwijdige geulen* (Tech. Rep. No. H1828). Retrieved 2024-04-04, from https://repository.tudelft.nl/islandora/object/uuid%3A3afdbae5-f4cc-4ad3-a5f2-2445a7e696dc (Publisher: Deltares (WL))

Arcadis. (2011, December). *Afleidingen Hydromorfologie Rijkswateren* (Tech. Rep.). Author. Retrieved from https://www.helpdeskwater.nl/publish/pages/130334/rapport_hydromorfologie_rijkswateren_23-12-2011.pdf

Auerbach, L. W., Goodbred, S. L., Mondal, D. R., Wilson, C. A., Ahmed, K. R., Roy, K., ... Ackerly, B. A. (2015). Flood risk of natural and embanked landscapes on the Ganges-Brahmaputra tidal delta plain. *Nature Climate Change*, *5*(2), 153–157. doi: 10.1038/nclimate2472

Bain, R. L., Hale, R. P., & Goodbred, S. L. (2019). Flow Reorganization in an Anthropogenically Modified Tidal Channel Network: An Example From the Southwestern Ganges-Brahmaputra-Meghna Delta. *Journal of Geophysical Research: Earth Surface*, *124*(8), 2141–2159. doi: 10.1029/2018JF004996

Bao, S., Zhang, W., Qin, J., Zheng, J., Lv, H., Feng, X., ... Hoitink, A. J. F. (2022). Peak Water Level Response to Channel Deepening Depends on Interaction Between Tides and the River Flow. *Journal of Geophysical Research: Oceans*, *127*(4), e2021JC017625. Retrieved 2024-03-04, from https://onlinelibrary.wiley.com/doi/abs/10.1029/2021JC017625 (_eprint: https://onlinelibrary.wiley.com/doi/pdf/10.1029/2021JC017625)

549 doi: 10.1029/2021JC017625
550 Beets, D. J., van der Valk, L., & Stive, M. J. F. (1992, January). Holocene evo-
551 lution of the coast of Holland. *Marine Geology*, *103*(1), 423–443. Retrieved
552 2024-02-28, from https://www.sciencedirect.com/science/article/pii/
553 002532279290030L doi: 10.1016/0025-3227(92)90030-L
554 Behre, K.-E. (1999, January). Die Veränderung der niedersächischen Küstenlinien in
555 den letzten 3000 Jahren und ihre Ursachen. *Probleme der Küstenforschung im*
556 *südlichen Nordseegebiet*, *26*, 9–33.
557 Borchert, S. M., Osland, M. J., Enwright, N. M., & Griffith, K. T. (2018).
558 Coastal wetland adaptation to sea level rise: Quantifying potential
559 for landward migration and coastal squeeze. *Journal of Applied*
560 *Ecology*, *55*(6), 2876–2887. Retrieved 2024-03-28, from https://
561 onlinelibrary.wiley.com/doi/abs/10.1111/1365-2664.13169 (_eprint:
562 https://onlinelibrary.wiley.com/doi/pdf/10.1111/1365-2664.13169) doi:
563 10.1111/1365-2664.13169
564 Braat, L., Van Kessel, T., Leuven, J. R., & Kleinhans, M. G. (2017). Effects
565 of mud supply on large-scale estuary morphology and development over
566 centuries to millennia. *Earth Surface Dynamics*, *5*(4), 617–652. doi:
567 10.5194/esurf-5-617-2017
568 Chen, L., Zhou, Z., Xu, F., Jimenez, M., Tao, J., & Zhang, C. (2020, January).
569 Simulating the impacts of land reclamation and de-reclamation on the morpho-
570 dynamics of tidal networks. *Anthropocene Coasts*, *3*(1), 30–42. Retrieved 2023-
571 08-17, from https://cdnsciencepub.com/doi/full/10.1139/anc-2019-0010
572 (Publisher: NRC Research Press) doi: 10.1139/anc-2019-0010
573 Coco, G., Zhou, Z., van Maanen, B., Olabarrieta, M., Tinoco, R., & Townend, I.
574 (2013). Morphodynamics of tidal networks: Advances and challenges. *Marine*
575 *Geology*, *346*, 1–16. Retrieved from http://dx.doi.org/10.1016/j.margeo
576 .2013.08.005 (Publisher: Elsevier B.V.) doi: 10.1016/j.margeo.2013.08.005
577 Cox, T., Maris, T., De Vleeschauwer, P., De Mulder, T., Soetaert, K., & Meire,
578 P. (2006, November). Flood control areas as an opportunity to restore
579 estuarine habitat. *Ecological Engineering*, *28*(1), 55–63. Retrieved 2024-
580 03-04, from https://www.sciencedirect.com/science/article/pii/
581 S0925857406000735 doi: 10.1016/j.ecoleng.2006.04.001
582 Dai, Z., Fagherazzi, S., Mei, X., Chen, J., & Meng, Y. (2016). Linking the in-
583 filling of the North Branch in the Changjiang (Yangtze) estuary to anthro-
584 pogenic activities from 1958 to 2013. *Marine Geology*, *379*, 1–12. doi:
585 10.1016/j.margeo.2016.05.006
586 de Haas, T., Pierik, H. J., van der Spek, A. J., Cohen, K. M., van Maanen, B., &
587 Kleinhans, M. G. (2018). Holocene evolution of tidal systems in The Nether-
588 lands: Effects of rivers, coastal boundary conditions, eco-engineering species,
589 inherited relief and human interference. *Earth-Science Reviews*, *177*(October
590 2017), 139–163. Retrieved from https://doi.org/10.1016/j.earscirev
591 .2017.10.006 (Publisher: Elsevier) doi: 10.1016/j.earscirev.2017.10.006
592 De Jong, J. (2006). *Habitat Maps Ems Estuary and Historical Habitat Change*
593 (HARBASINS report). Assen: Ecca advies.
594 Donatelli, C., Ganju, N. K., Zhang, X., Fagherazzi, S., & Leonardi, N.
595 (2018). Salt Marsh Loss Affects Tides and the Sediment Bud-
596 get in Shallow Bays. *Journal of Geophysical Research: Earth Sur-*
597 *face*, *123*(10), 2647–2662. Retrieved 2023-07-31, from https://
598 onlinelibrary.wiley.com/doi/abs/10.1029/2018JF004617 (_eprint:
599 https://onlinelibrary.wiley.com/doi/pdf/10.1029/2018JF004617) doi:
600 10.1029/2018JF004617
601 Dronkers, J. (1986). Tidal asymmetry and estuarine morphology. *Netherlands Jour-*
602 *nal of Sea Research*, *20*(2-3), 117–131. doi: 10.1016/0077-7579(86)90036-0
603 Dronkers, J. (2016). *Dynamics of Coastal Systems*. WORLD SCIENTIFIC. Re-

trieved from https://www.worldscientific.com/doi/abs/10.1142/9818 doi: 10.1142/9818

D'Alpaos, A., Lanzoni, S., Marani, M., & Rinaldo, A. (2010, January). On the tidal prism—Channel area relations. *Journal of Geophysical Research*, *115*. doi: 10.1029/2008JF001243

Fortunato, A. B., & Oliveira, A. (2005). Influence of Intertidal Flats on Tidal Asymmetry. *Journal of Coastal Research*, *215*(215), 1062–1067. doi: 10.2112/03-0089.1

Friedrichs, C. T. (2010). *Barotropic tides in channelized estuaries.* (Publication Title: Contemporary Issues in Estuarine Physics Issue: January 2010) doi: 10.1017/CBO9780511676567.004

Friedrichs, C. T., & Aubrey, D. G. (1988). Nonlinear tidal distortion in shallow well-mixed estuaries. *Estuarine, Coastal and Shelf Science*, *30*(3), 321–322. (ISBN: 0272-7714) doi: 10.1016/0272-7714(90)90054-U

Gerritsen, F. (1952). *Historical and hydrographical investigations in the Ems estuary* (Tech. Rep.). Hoorn: Ministry of Public Works. Retrieved from https://open.rws.nl/open-overheid/onderzoeksrapporten/@91330/historisch-hydrografisch-onderzoek-eems/

Groen, P. (1967). On the residual transport of suspended matter by an alternating tidal current. *Netherlands Journal of Sea Research*, *3*(4), 564–574. doi: 10.1016/0077-7579(67)90004-X

Guo, L., Xie, W., Xu, F., Wang, X., Zhu, C., Meng, Y., ... He, Q. (2022). A historical review of sediment export–import shift in the North Branch of Changjiang Estuary. *Earth Surface Processes and Landforms*, *47*(1), 5–16. doi: 10.1002/esp.5084

Guo, L., Zhu, C., Xu, F., Xie, W., van der Wegen, M., Townend, I., ... He, Q. (2022). Reclamation of Tidal Flats Within Tidal Basins Alters Centennial Morphodynamic Adaptation to Sea-Level Rise. *Journal of Geophysical Research: Earth Surface*, *127*(6), 1–24. doi: 10.1029/2021jf006556

Herrling, G., & Niemeyer, H. D. (2007). Long-term Spatial Development of Habitats in the Ems-Dollard Estuary.

Herrling, G., & Niemeyer, H. D. (2008). Reconstruction of the historical tidal regime of the Ems-Dollard estuary prior to significant human changes by applying mathematical modeling.

Hiatt, M., & Passalacqua, P. (2015). Hydrological connectivity in river deltas: The first-order importance of channel-island exchange. *ater Resources Research*, *51*, 2264–2282. doi: 10.1111/j.1752-1688.1969.tb04897.x

Hibma, A., Schuttelaars, H. M., & De Vriend, H. J. (2004). Initial formation and long-term evolution of channel-shoal patterns. *Continental Shelf Research*, *24*(15), 1637–1650. doi: 10.1016/j.csr.2004.05.003

Hibma, a., Stive, M., & Wang, Z. (2004, October). Estuarine morphodynamics. *Coastal Engineering*, *51*(8-9), 765–778. Retrieved 2015-01-14, from http://linkinghub.elsevier.com/retrieve/pii/S037838390400081X doi: 10.1016/j.coastaleng.2004.07.008

Hoitink, A. J., Nittrouer, J. A., Passalacqua, P., Shaw, J. B., Langendoen, E. J., Huismans, Y., & van Maren, D. S. (2020). Resilience of River Deltas in the Anthropocene. *Journal of Geophysical Research: Earth Surface*, *125*(3), 1–24. doi: 10.1029/2019JF005201

Homeier, H. (1962). *Historisches Kartenwerk 1:50 000 der niedersächsischen Küste* (Tech. Rep.).

Homeier, H., Siebert, E., & Kramer, J. (1969). *Der Gestaltwandel der ostfriesischen Küste im Laufe der Jahrhunderte: ein Jahrtausend ostfriesischer Deichgeschichte. Entwicklung des Deichwesens vom Mittelalter bis zur Gegenwart.* Deichamt Krummhörn. (Google-Books-ID: w6ikPQAACAAJ)

Jarrett, J. (1976). Tidal prism-inlet area relationships General investigation of tidal

inlets. (3).

Jeuken, M. C., & Wang, Z. B. (2010). Impact of dredging and dumping on the stability of ebb-flood channel systems. *Coastal Engineering*, *57*(6), 553–566. Retrieved from http://dx.doi.org/10.1016/j.coastaleng.2009.12.004 (Publisher: Elsevier B.V.) doi: 10.1016/j.coastaleng.2009.12.004

Kleinhans, M. G., Roelofs, L., Weisscher, S. A. H., Lokhorst, I. R., & Braat, L. (2022). Estuarine morphodynamics and development modified by floodplain formation. , 367–381. Retrieved from https://doi.org/10.5194/esurf-2021-75

Knottnerus, O. S. (2013a). Dollardgeschiedenis(sen) - Mythe en realiteit. In: K. Essink (Red.), Stormvloed 1509 - Geschiedenis van de Dollard. In (pp. 95–116). Groningen: Stichting Verdronken Geschiedenis.

Knottnerus, O. S. (2013b, January). Reclamations and submerged lands in the Ems River Estuary (900–1500). In *Landscapes or seascapes? The history of the coastal environment in the North Sea area reconsidered.* (pp. 241–266). CORN Publication Series. doi: 10.1484/M.CORN.1.101555

Lang, A. W. (1954). *Untersuchung zum Gestaltungswandel des Emsmündungstrichters* (Tech. Rep.).

Leuven, J. R., & Kleinhans, M. G. (2019). Incipient Tidal Bar and Sill Formation. *Journal of Geophysical Research: Earth Surface*, *124*(7), 1762–1781. doi: 10.1029/2018JF004953

Liu, J., Dietz, T., Carpenter, S. R., Alberti, M., Folke, C., Moran, E., ... Taylor, W. W. (2007, September). Complexity of Coupled Human and Natural Systems. *Science*, *317*(5844), 1513–1516. Retrieved 2023-10-23, from https://www.science.org/doi/10.1126/science.1144004 (Publisher: American Association for the Advancement of Science) doi: 10.1126/science.1144004

Monge-Ganuzas, M., Cearreta, A., & Evans, G. (2013, June). Morphodynamic consequences of dredging and dumping activities along the lower Oka estuary (Urdaibai Biosphere Reserve, southeastern Bay of Biscay, Spain). *Ocean & Coastal Management*, *77*, 40–49. Retrieved 2023-10-12, from https://www.sciencedirect.com/science/article/pii/S0964569112000270 doi: 10.1016/j.ocecoaman.2012.02.006

O'Brien, & P., M. (1931). Estuary tidal prisms related to entrance areas. *Civil Engineering*. Retrieved 2020-10-21, from http://ci.nii.ac.jp/naid/10016529954/en/

Olds, A., Nagelkerken, I., Huijbers, C., Gilby, B., Pittman, S., & Schlacher, T. (2017). Connectivity in coastal seascapes. In *Seascape Ecology* (pp. pp. 261–292). John Wiley & Sons Ltd.

Pierik, H. (2019). *GIS dataset historical bathymetry and resistant layers in the Ems-Dollard estuary.* DANS. Retrieved from https://easy.dans.knaw.nl/ui/datasets/id/easy-dataset:118303/tab/1 (Place: Utrecht) doi: 10.17026/dans-x8w-wzsj

Pierik, H. J., Leuven, J. R. F. W., Busschers, F. S., Hijma, M., & Kleinhans, M. G. (2022). Depth-limiting resistant layers restrict dimensions and positions of estuarine channels and bars. *Depositional Record*(February), 1–20. doi: 10.1002/dep2.184

Ralston, D. K., Talke, S., Geyer, W. R., Al-Zubaidi, H. A. M., & Sommerfield, C. K. (2019). Bigger Tides, Less Flooding: Effects of Dredging on Barotropic Dynamics in a Highly Modified Estuary. *Journal of Geophysical Research: Oceans*, *124*(1), 196–211. Retrieved 2024-03-06, from https://onlinelibrary.wiley.com/doi/abs/10.1029/2018JC014313 (_eprint: https://onlinelibrary.wiley.com/doi/pdf/10.1029/2018JC014313) doi: 10.1029/2018JC014313

Ridderinkhof, W., de Swart, H. E., van der Vegt, M., Alebregtse, N. C., & Hoekstra,

P. (2014). Geometry of tidal inlet systems: A key factor for the net sediment transport in tidal inlets W. *Journal of Geophysical Research: Oceans*(119), 3868–3882. Retrieved from http://onlinelibrary.wiley.com/doi/10.1002/jgrc.20353/abstract doi: 10.1002/2014JC010226.Received

Schrijvershof, R. (2024, April). *Geospatial datasets of land reclamation and morphological reconstructions of the Ems estuary since the 16th century.* [object Object]. Retrieved 2024-04-09, from https://data.4tu.nl/datasets/78ac0cf9-e9f7-47c7-8c4e-93f7fb2c633e/1 doi: 10.4121/78AC0CF9-E9F7-47C7-8C4E-93F7FB2C633E.V1

Siemes, R. W. A., Duong, T. M., Willemsen, P. W. J. M., Borsje, B. W., & Hulscher, S. J. M. H. (2023, November). Morphological Response of a Highly Engineered Estuary to Altering Channel Depth and Restoring Wetlands. *Journal of Marine Science and Engineering*, *11*(11), 2150. Retrieved 2024-03-06, from https://www.mdpi.com/2077-1312/11/11/2150 (Number: 11 Publisher: Multidisciplinary Digital Publishing Institute) doi: 10.3390/jmse11112150

Sievers, J., Milbradt, P., Ihde, R., Valerius, J., Hagen, R., & Plüß, A. (2021, August). An integrated marine data collection for the German Bight – Part 1: Subaqueous geomorphology and surface sedimentology (1996–2016). *Earth System Science Data*, *13*(8), 4053–4065. Retrieved 2023-06-08, from https://essd.copernicus.org/articles/13/4053/2021/ (Publisher: Copernicus GmbH) doi: 10.5194/essd-13-4053-2021

Speer, P. E., & Aubrey, D. G. (1985). A Study of Non-linear Tidal Propagation in Shallow Inlet/Estuarine Systems Part II: Theory". *Estuarine, Coastal and Shelf Science*, *21*(5691), 207–224.

Stive, M. J. F., & Wang, Z. B. (2003, January). Chapter 13 Morphodynamic modeling of tidal basins and coastal inlets. In V. C. Lakhan (Ed.), *Elsevier Oceanography Series* (Vol. 67, pp. 367–392). Elsevier. Retrieved 2024-04-02, from https://www.sciencedirect.com/science/article/pii/S0422989403801307 doi: 10.1016/S0422-9894(03)80130-7

Stratingh, G. A., & Venema, G. A. (1855). *De Dollard of Geschied,- Aardrijks- en Natuurkundige Beschrijving van dezen Boezem der Eems.* Winschoten.

Talke, S. A., & Jay, D. A. (2020). Changing Tides: The Role of Natural and Anthropogenic Factors. *Annual Review of Marine Science*, *12*(1), 121–151. Retrieved 2023-04-24, from https://doi.org/10.1146/annurev-marine-010419-010727 (_eprint: https://doi.org/10.1146/annurev-marine-010419-010727) doi: 10.1146/annurev-marine-010419-010727

Van de Kreeke, J., & Robaczewska, K. (1993). Tide-induced residual transport of coarse sediment; Application to the EMS estuary. *Netherlands Journal of Sea Research*, *31*(3), 209–220. doi: 10.1016/0077-7579(93)90022-K

van der Molen, J., & de Swart, H. E. (2001). Holocene tidal conditions and tide-induced sand transport in the southern North Sea. *Journal of Geophysical Research: Oceans*, *106*(C5), 9339–9362. Retrieved 2024-03-07, from https://onlinelibrary.wiley.com/doi/abs/10.1029/2000JC000488 (_eprint: https://onlinelibrary.wiley.com/doi/pdf/10.1029/2000JC000488) doi: 10.1029/2000JC000488

van der Spek, A. J. (1994). *Large-scale evolution of holocene tidal basins in the Netherlands.*

Van Der Wegen, M. (2013). Numerical modeling of the impact of sea level rise on tidal basin morphodynamics. *Journal of Geophysical Research: Earth Surface*, *118*(2), 447–460. doi: 10.1002/jgrf.20034

van der Wegen, M., Wang, Z. B., Savenije, H. H. G., & Roelvink, J. A. (2008). Long-term morphodynamic evolution and energy dissipation in a coastal plain, tidal embayment. *Journal of Geophysical Research: Earth Surface*, *113*(F3). Retrieved 2024-03-28, from https://

onlinelibrary.wiley.com/doi/abs/10.1029/2007JF000898 (_eprint: https://onlinelibrary.wiley.com/doi/pdf/10.1029/2007JF000898) doi: 10.1029/2007JF000898

van Dijk, W. M., Cox, J. R., Leuven, J. R., Cleveringa, J., Taal, M., Hiatt, M. R., ... Kleinhans, M. G. (2021). The vulnerability of tidal flats and multi-channel estuaries to dredging and disposal. *Anthropocene Coasts*, *4*(1), 36–60. doi: 10.1139/anc-2020-0006

van Maren, D. S., Beemster, J., Wang, Z., Khan, Z. H., Schrijvershof, R., & Hoitink, A. (2023). Tidal Amplification and River Capture in Response to Asynchronous Land Reclamation in the Ganges-Brahmaputra Delta. *Catena*, *220*(PA), 106651. Retrieved from https://doi.org/10.1016/j.catena.2022.106651 (Publisher: Elsevier B.V.) doi: 10.2139/ssrn.4064791

van Maren, D. S., Colina Alonso, A., Engels, A., Vandenbruwaene, W., de Vet, P. L. M., Vroom, J., & Wang, Z. B. (2023). Adaptation timescales of estuarine systems to human interventions. *Frontiers in Earth Science*, *11*. Retrieved 2023-05-16, from https://www.frontiersin.org/articles/10.3389/feart.2023.1111530

Van Maren, D. S., Oost, A. P., Wang, Z. B., & Vos, P. C. (2016). The effect of land reclamations and sediment extraction on the suspended sediment concentration in the Ems Estuary. *Marine Geology*, *376*, 147–157. Retrieved from http://dx.doi.org/10.1016/j.margeo.2016.03.007 (Publisher: The Authors) doi: 10.1016/j.margeo.2016.03.007

Van Maren, D. S., van Kessel, T., Cronin, K., & Sittoni, L. (2015). The impact of channel deepening and dredging on estuarine sediment concentration. *Continental Shelf Research*, *95*, 1–14. Retrieved from http://dx.doi.org/10.1016/j.csr.2014.12.010 (Publisher: Elsevier) doi: 10.1016/j.csr.2014.12.010

Van Maren, D. S., Winterwerp, J. C., & Vroom, J. (2015). Fine sediment transport into the hyper-turbid lower Ems River: the role of channel deepening and sediment-induced drag reduction. *Ocean Dynamics*, *65*(4), 589–605. (ISBN: 1023601508) doi: 10.1007/s10236-015-0821-2

Van Veen, J. (1950). Eb- en Vloedschaar Systemen in de Nederlandse Getijwateren. *Journal of the Royal Dutch Geographical Society*, *67*(November), 303–325.

Van Veen, J., van der Spek, A. J. F., Stive, M. J. F., & Zitman, T. (2005). Ebb and Flood Channel Systems in the Netherlands Tidal Waters. *Journal of Coastal Research*, *216*(November), 1107–1120. doi: 10.2112/04-0394.1

Vellinga, N. E., Hoitink, A. J., van der Vegt, M., Zhang, W., & Hoekstra, P. (2014). Human impacts on tides overwhelm the effect of sea level rise on extreme water levels in the Rhine-Meuse delta. *Coastal Engineering*, *90*, 40–50. Retrieved from http://dx.doi.org/10.1016/j.coastaleng.2014.04.005 (Publisher: Elsevier B.V.) doi: 10.1016/j.coastaleng.2014.04.005

Voorsmit, O. V. (2006, April). *Het meergeulenstelsel van de Westerschelde en de relatie met de functies van de Langetermijnvisie : een kritische analyse van het beleidsuitgangspunt 'Instandhouding van het meergeulenstelsel van de Westerschelde'* [info:eu-repo/semantics/masterThesis]. Retrieved 2024-04-02, from https://essay.utwente.nl/56958/ (Publisher: University of Twente)

Vos, P., Van der Meulen, M., Weerts, H., & Bazelmans, J. (2020). *Atlas of the Holocene Netherlands: Landscape and Habitation since the Last Ice Age.* doi: 10.5117/9789463724432

Vos, P., & van Kesteren, W. (2000, September). The long-term evolution of intertidal mudflats in the northern Netherlands during the Holocene; natural and anthropogenic processes. *Continental Shelf Research*, *20*, 1687–1710. doi: 10.1016/S0278-4343(00)00043-1

Vos, P. C., & Knol, E. (2013). De ontstaansgeschiedenis van het Dollardlandschap; natuurlijke en antropogene processen. In: K. Essink (Red.), Stormvloed 1509 -

Geschiedenis van de Dollard. Groningen: Stichting Verdronken Geschiedenis.

Vos, P. C., & Knol, E. (2015). Holocene landscape reconstruction of the Wadden Sea area between Marsdiep and Weser. *Geologie en Mijnbouw/Netherlands Journal of Geosciences*, *94*(2), 157–183. doi: 10.1017/njg.2015.4

Wang, Z., Jeuken, C., & Vriend, H. d. (1999). *Tidal asymmetry and residual sediment transport in estuaries* (Tech. Rep.). WL | Delft hydraulics. (Issue: November)

Wang, Z. B., Van Maren, D. S., Ding, P. X., Yang, S. L., Van Prooijen, B. C., De Vet, P. L., ... He, Q. (2015). Human impacts on morphodynamic thresholds in estuarine systems. *Continental Shelf Research*, *111*, 174–183. doi: 10.1016/j.csr.2015.08.009

Wang, Z. B., & Winterwerp, H. (2001, September). Impact of Dredging and Dumping on the Stability of Ebb-Flood Channel Systems..

Weisscher, S. A., Baar, A. W., van Belzen, J., Bouma, T. J., & Kleinhans, M. G. (2022). Transitional polders along estuaries: Driving land-level rise and reducing flood propagation. *Nature-Based Solutions*, *2*(June), 100022. Retrieved from `https://doi.org/10.1016/j.nbsj.2022.100022` (Publisher: Elsevier Inc.) doi: 10.1016/j.nbsj.2022.100022

Wilson, C., Goodbred, S., Small, C., Gilligan, J., Sams, S., Mallick, B., & Hale, R. (2017). Widespread infilling of tidal channels and navigable waterways in the human-modified tidal deltaplain of southwest Bangladesh. *Elementa*, *5*. doi: 10.1525/elementa.263

Winterwerp, J. C., Wang, Z. B., Van Braeckel, A., Van Holland, G., & Kösters, F. (2013). Man-induced regime shifts in small estuaries - II: A comparison of rivers. *Ocean Dynamics*, *63*(11-12), 1293–1306. doi: 10.1007/s10236-013-0663-8

Zhou, Z., Coco, G., Townend, I., Gong, Z., Wang, Z., & Zhang, C. (2018). On the stability relationships between tidal asymmetry and morphologies of tidal basins and estuaries. *Earth Surface Processes and Landforms*, *43*(9). doi: 10.1002/esp.4366

Zhu, C., Guo, L., van Maren, D. S., Tian, B., Wang, X., He, Q., & Wang, Z. B. (2019). Decadal morphological evolution of the mouth zone of the Yangtze Estuary in response to human interventions. *Earth Surface Processes and Landforms*, *44*(12), 2319–2332. Retrieved 2023-10-12, from `https://onlinelibrary.wiley.com/doi/abs/10.1002/esp.4647` (_eprint: https://onlinelibrary.wiley.com/doi/pdf/10.1002/esp.4647) doi: 10.1002/esp.4647

Figure 01.

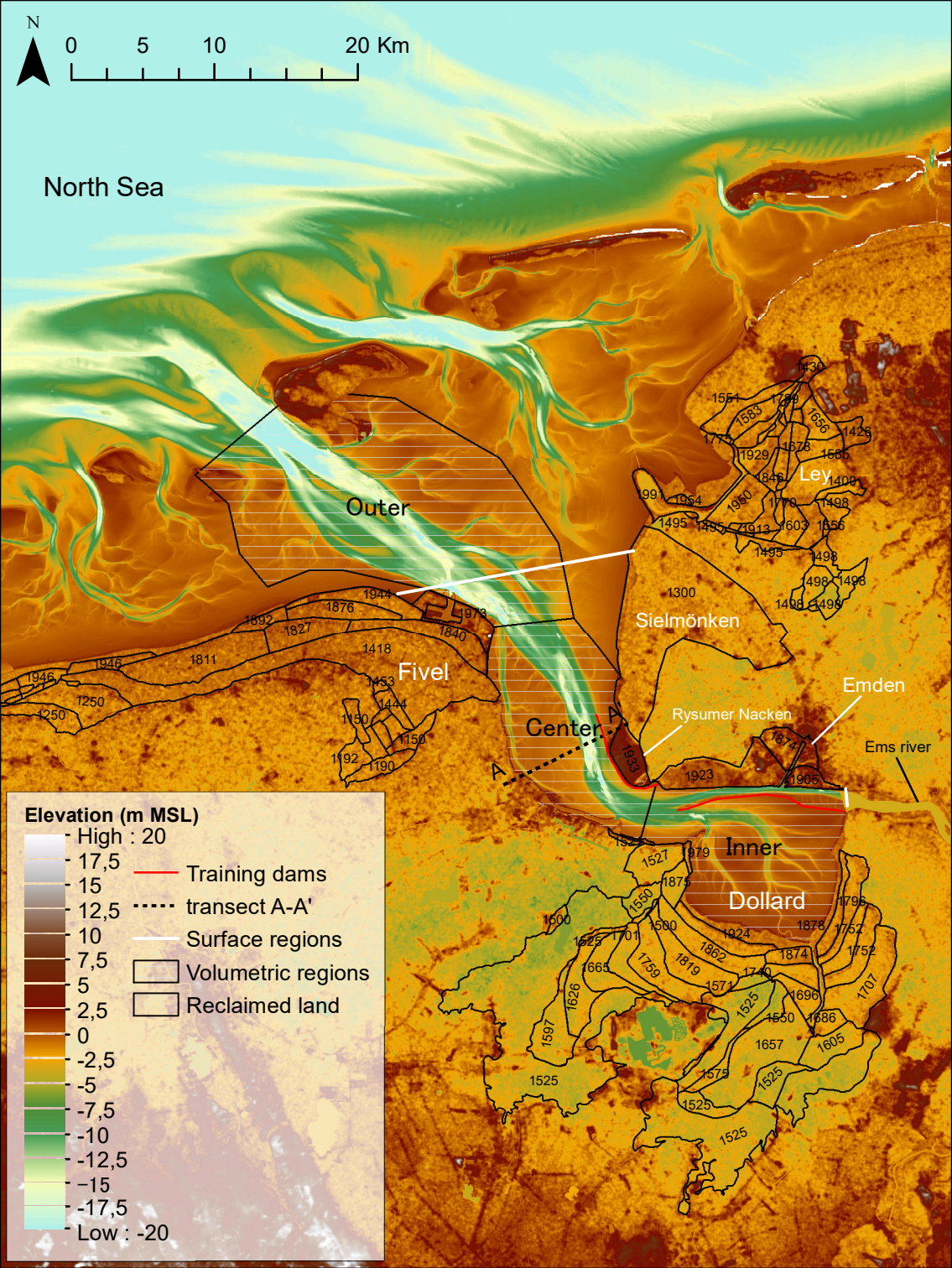
N
0
5
10
20 Km
North Sea
Outer
Fivel
Center
Sielmönken
Ley
Emden
Rysumer Nacken
Ems river
Inner
Dollard
A
A
Elevation (m MSL)
High : 20
17,5
15
12,5
10
7,5
5
2,5
0
-2,5
-5
-7,5
-10
-12,5
−15
-17,5
Low : -20
Training dams
transect A-A'
Surface regions
Volumetric regions
Reclaimed land

Figure 02.

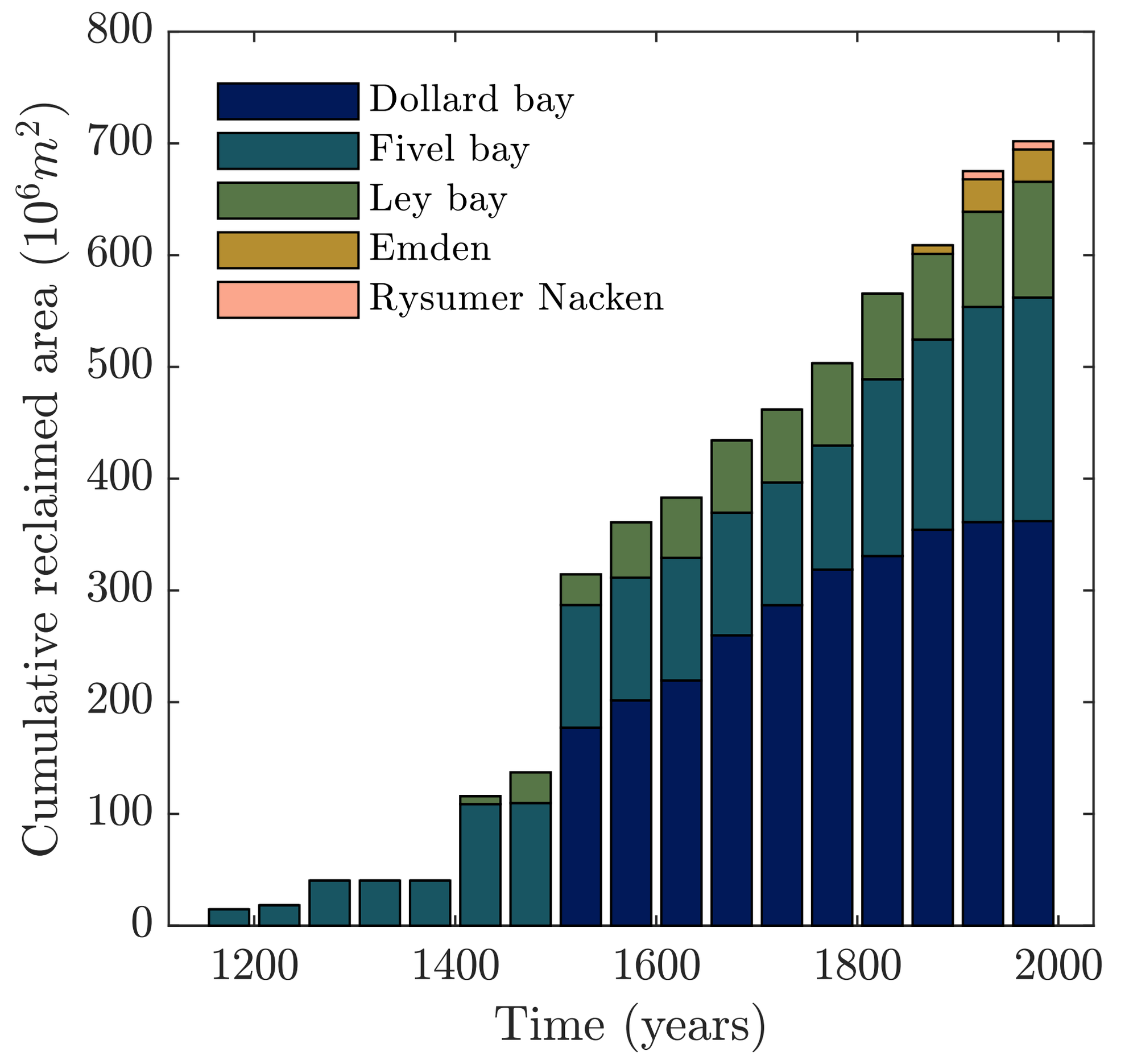
Dollard bay
Fivel bay
Ley bay
Emden
Rysumer Nacken
Cumulative reclaimed area ($10^6 m^2$)
0
100
200
300
400
500
600
700
800
1200
1400
1600
1800
2000
Time (years)

Figure 03.

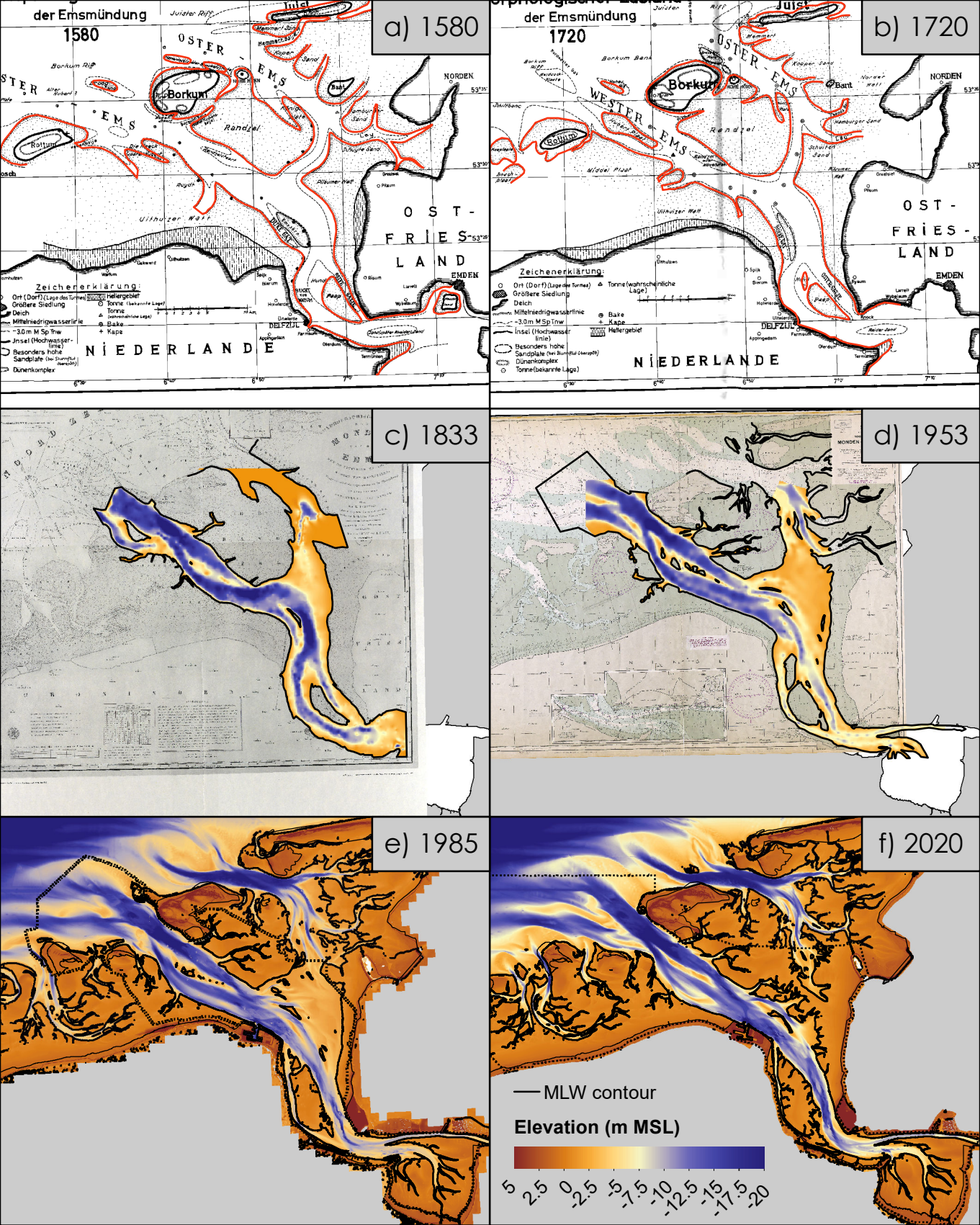
a) 1580
der Emsmündung
1580
b) 1720
der Emsmündung
1720
Borkum
Juist
NORDEN
EMDEN
DELFZIJL
OST-
FRIES-
LAND
NIEDERLANDE
Zeichenerklärung:
c) 1833
d) 1953
e) 1985
f) 2020
MLW contour
Elevation (m MSL)
5
2.5
0
-2.5
-5
-7.5
-10
-12.5
-15
-17.5
-20

Figure 04.

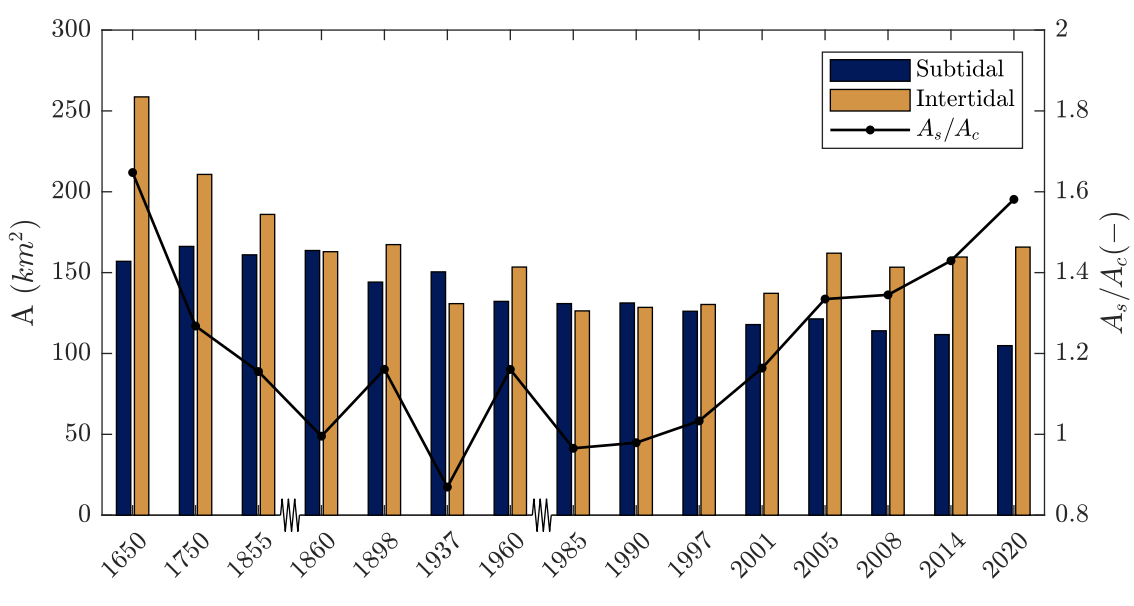
Subtidal
Intertidal
A_s/A_c
A (km^2)
$A_s/A_c(-)$
300
250
200
150
100
50
0
2
1.8
1.6
1.4
1.2
1
0.8
1650
1750
1855
1860
1898
1937
1960
1985
1990
1997
2001
2005
2008
2014
2020

Figure 05.

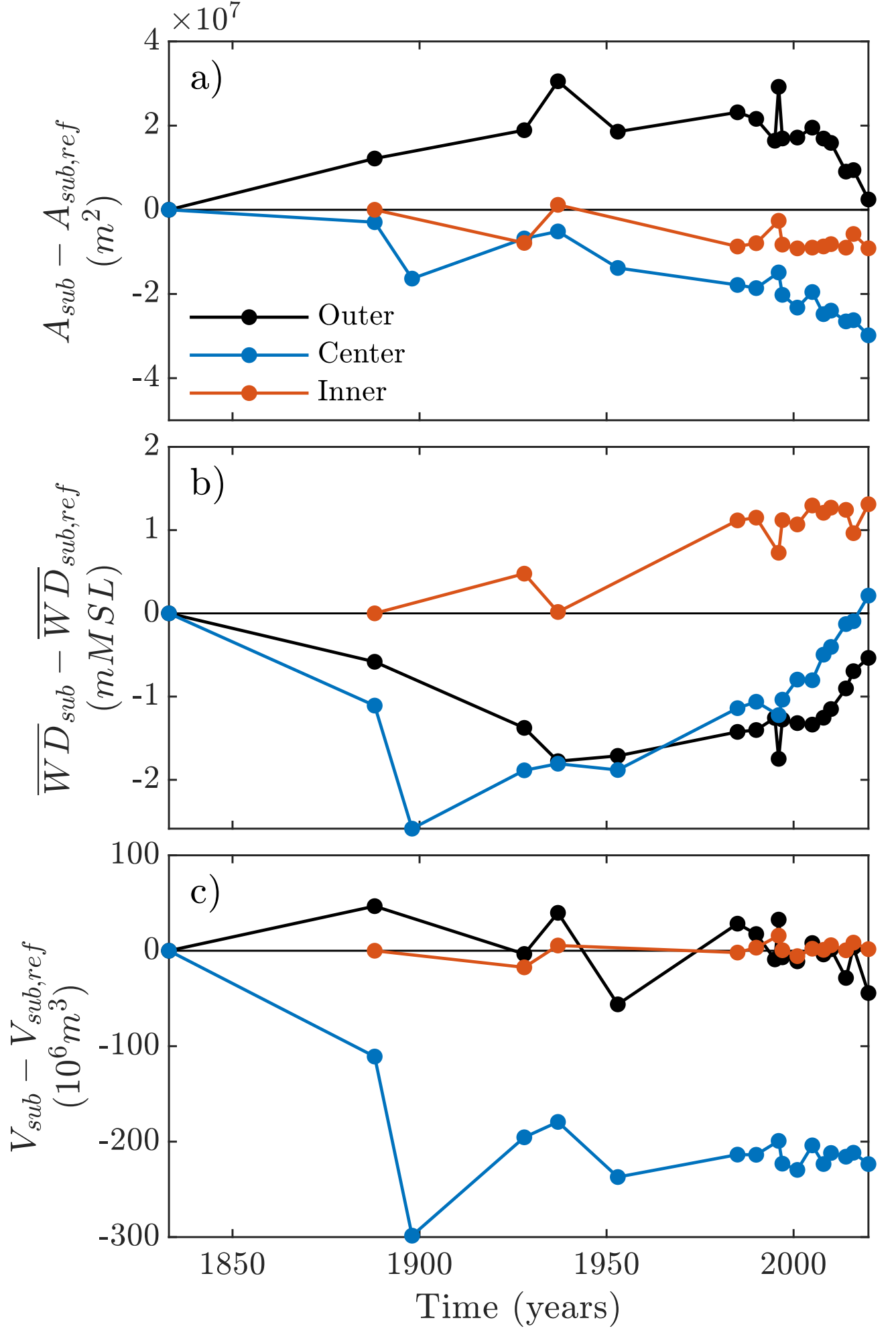
×10^7
4
2
0
-2
-4
a)
$A_{sub} - A_{sub,ref}$ (m^2)
Outer
Center
Inner
2
1
0
-1
-2
b)
$\overline{WD}_{sub} - \overline{WD}_{sub,ref}$ $(m MSL)$
100
0
-100
-200
-300
c)
$V_{sub} - V_{sub,ref}$ $(10^6 m^3)$
1850
1900
1950
2000
Time (years)

Figure 06.

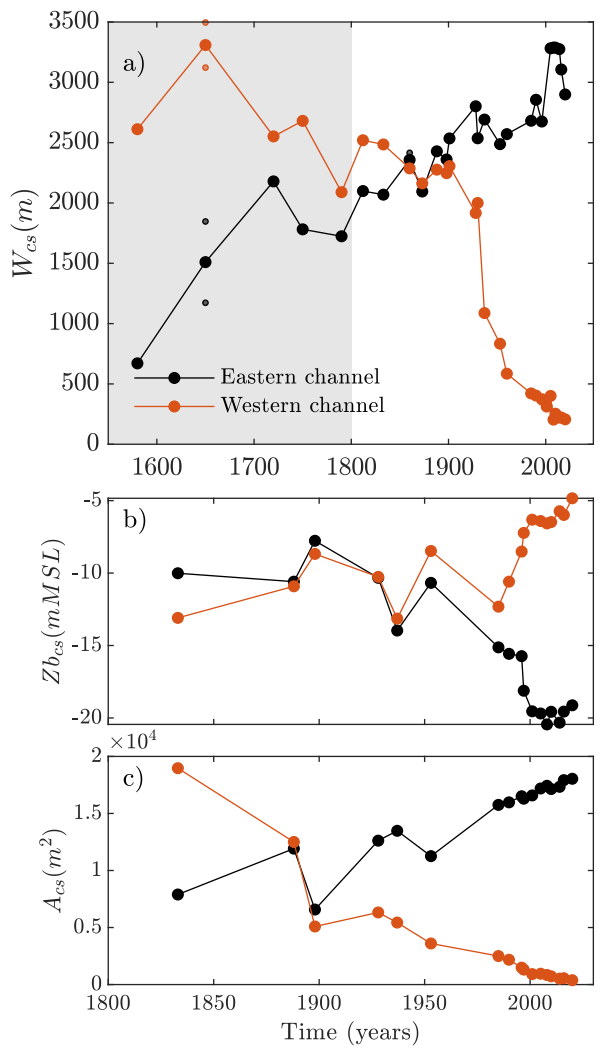
a)
$W_{cs}(m)$
3500
3000
2500
2000
1500
1000
500
0
Eastern channel
Western channel
1600
1700
1800
1900
2000
b)
$Zb_{cs}(mMSL)$
-5
-10
-15
-20
c)
$\times 10^4$
$A_{cs}(m^2)$
2
1.5
1
0.5
0
1800
1850
1900
1950
2000
Time (years)

Figure 07.

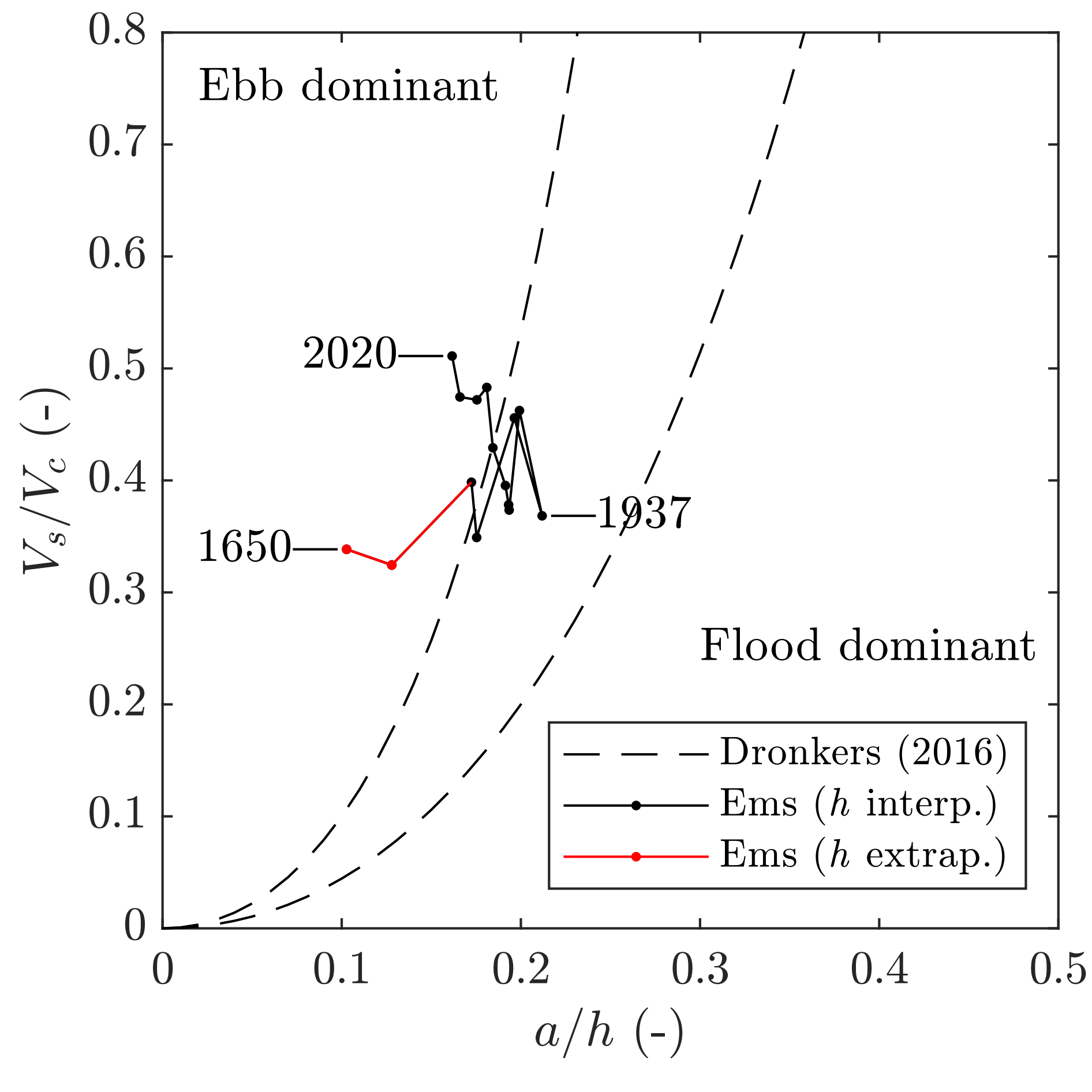
Ebb dominant
Flood dominant
2020
1937
1650
Dronkers (2016)
Ems (h interp.)
Ems (h extrap.)
V_s/V_c (-)
a/h (-)
0
0.1
0.2
0.3
0.4
0.5
0.6
0.7
0.8